Journal of Asian Concrete Federation
Vol. 9, No. 1, pp. 65-102, June. 2023
ISSN 2465-7964 / eISSN 2465-7972
DOI http://dx.doi.org/10.18702/acf.2023.9.1.65

Review Paper

Fire Performance of Fiber-reinforced Ultra-High-Performance Concrete: A state-of-the-art review

Mehran Khan, Mingfeng Kai*, Muhammad Ahmad, Jiancong Lao, Jian-Guo Dai
(Received: April 12, 2023; Revised: April 24, 2023, Accepted: May 6, 2023; Published online: June 30, 2023)

Abstract: Explosive spalling is a major problem for structures made of ultra-high-performance concrete (UHPC) after being exposed to fire, which hinders their practical applications. To overcome this obstacle, fibers have become an essential constituent of UHPC in past decades. This paper summarizes a state-of-the-art review related to the fire performance of UHPC using single and hybrid fibers. The spalling behavior, spalling mechanism, mechanical properties, and microstructure characteristics of fiber-reinforced UHPC are summarized, and structural performance of fiber-reinforced UHPC members at elevated temperatures is discussed. This review reveals that fire-induced spalling is a significant concern in UHPC, and it can be caused by various mechanisms. The addition of fibers can play a crucial role in preventing spalling, and different mechanisms for different types of fibers have been reported in the literature for UHPC with both single and hybrid fibers. Therefore, fiber hybridization is recommended to enhance the spalling resistance of UHPC. The future directions and challenges for UHPC at both the material and structural levels are discussed.

Keywords: UHPC, Spalling behavior, Spalling mechanism, Mechanical properties, Microstructure, Structural performance, Fiber hybridization, Fire resistance.

Table of content

***Corresponding author Mingfeng Kai** *is a Research Assistant Professor at Department of Civil and Environmental Engineering, The Hong Kong Polytechnic University, Hong Kong, China*

Mehran Khan *is a Postdoctoral Researcher at Department of Civil and Environmental Engineering, The Hong Kong Polytechnic University, Hong Kong, China.*

Muhammad Riaz Ahmad *is a Research Assistant Professor at Department of Civil and Environmental Engineering, The Hong Kong Polytechnic University, Hong Kong, China*

Jiancong Lao *is a Researcher at Department of Civil and Environmental Engineering, The Hong Kong Polytechnic University, Hong Kong, China*

Jian-Guo Dai *is a Professor at Department of Civil and Environmental Engineering, The Hong Kong Polytechnic University, Hong Kong, China.*

1. Introduction

Ultra-high-performance concrete (UHPC) has gained significant attention and recognition as a sustainable infrastructure material in various countries including China, USA, Australia, France, and Europe [1-7]. The excellent mechanical

properties of UHPC are achieved by the elimination of coarse aggregate through the use of ultra-fine cementitious materials, resulting in a minimized void and microcracks. UHPC requires a higher cement content, fine quartz sand, micro silica, a higher quantity of superplasticizer, and a relatively low water to binder ratio [8, 9]. In the development of UHPC, the addition of micro silica (25-30%) creates a dense and impermeable microstructure, while crushed quartz sand serves as fine aggregate (<10μm), and coarse aggregate is replaced by fine quartz sand (150-600μm) [10]. UHPC typically exhibits good flowability (⩾ 160 mm), high compressive strength (⩾ 120 MPa) and tensile strength (⩾5 MPa), low permeability, and excellent durability due to its high particle packing density (0.825-0.855), low water to binder (w/b) ratio (0.15-0.25), and appropriate chemical admixtures [11-13]. As a result, UHPC has been increasingly used in various civil engineering constructions such as high-rise buildings, bridges, building facades, wind turbine towers, industrial floors, prefabricated prestressed girders, and permanent formwork [14, 15]. Moreover, UHPC's utilization as a structural concrete requires resistance to high temperatures, whether due to natural or accidental fires. This highlights the importance of considering fire resistance in UHPC's design and specification, to ensure that it maintains its structural integrity and continues to meet the required safety standards.

However, compared to normal concrete (having compressive strength of around 20-40 MPa), UHPC is more susceptible to explosive spalling (a term used to describe the sudden chipping of fragments from concrete surface) under high temperature [16, 17]. Usually, the explosive spalling of UHPC will happen when the temperature reaches ~ 300°C. Previously, two typical hypotheses were proposed to explain the explosive spalling of UHPC:(i) The first theory proposes that pore pressure is the major cause of the explosive spalling of UHPC. Pore pressure is built up due to moisture migration up to 320°C. Moisture in concrete is available in a different form [18] (i.e., free, adsorbed, and bonded) as shown in *Fig. 1*. In stage I (from 30 to 100 ^{o}C), the moisture is attributed to the evaporation of free water. In stage II (from 100 to 300 ^{o}C), the moisture is contributed by the free water, adsorbed water, some chemically bounded water, and inter-layered water from C-S-H gel. In stage III (from 300 to 500 ^{o}C), the moisture is caused by the decomposition of Ca $(OH)_2$ which is converted to CaO and H_2O. In stage IV (from 500 to 700 ^{o}C), the small amount of moisture left in C-S-H layers will be further released due to the decomposition of C-S-H; (ii) The second theory implies that the thermally induced stress is the primary cause of spalling under high temperature [19]. The thermally induced stresses occurred due to difference between the surface and internal temperature of UHPC under elevated temperature. Some studies considered that pore pressure and thermally induced stress work together to account for spalling [19]. Till now, there still exists debate about which one is the major cause for the explosive spalling of UHPC. According to the spalling temperature (refer to Fig. 2), the spalling can be classified in three types [19]: thermo-hydral, thermo-mechanical spalling, and thermo-chemical spalling:

(1) Thermo-hydral spalling: It occurs between 220-320°C due to thermally induced stress and/or pore pressure. This type of spalling is caused by the expansion of evaporated pore water due to the temperature rise, resulting in increased internal pressure, which can lead to cracking and spalling. At this stage, a portion of the C-S-H dehydrates.

(2) Thermo-mechanical spalling: It occurs between 430-460°C because of thermally induced stresses and/or applied mechanical stresses/driving forces. The mechanical stresses can be caused due to several factors, such as bending in longitudinal reinforcement, matrix volumetric expansion, and compressive stress exerted on the cracked beam/column cover. These factors can cause high tensile stresses in the concrete, leading to spalling. Between 400-550°C, calcium hydroxide ($Ca(OH)_2$) dissociate.

(3) Thermo-chemical spalling. It occurs due to thermally induced stresses and/or destruction of aggregate cement bonds at high temperatures (700-900°C). At such high temperatures, the aggregate expands, and the cement paste shrinks, weakening the bond between the paste and the aggregate. The disassociation of $Ca(OH)_2$ and C-S-H can also reduce the cement-aggregate bond and contribute to spalling. Finally, between 700-900°C, $CaCO_3$ dissociates, and the C-S-H transforms into wollastonite. Concrete subjected to such high temperatures (>900°C) may no longer be useful as the structural material and may require repair or replacement.

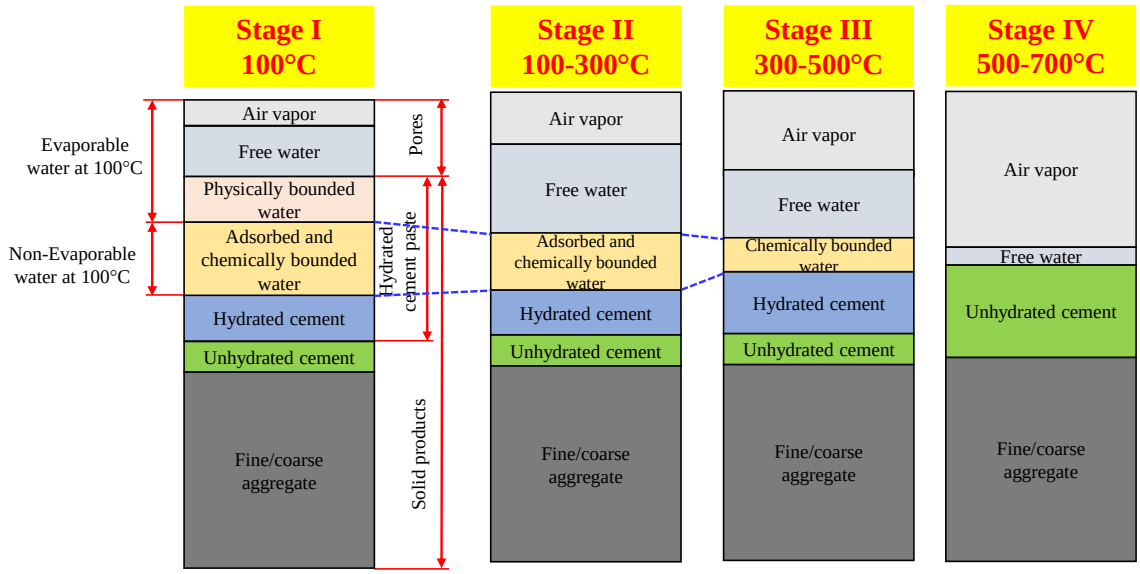

Fig. 1 – Types of water related to the UHPC constituents with an increase in temperature

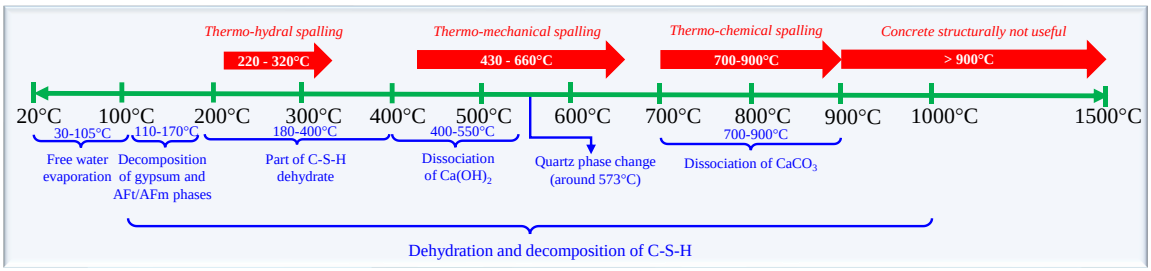

Fig. 2 – Types of spalling under elevated temperatures

The widely accepted method for preventing the spalling of UHPC is the addition of various types of fibers, such as steel fibers, polymer fibers (e.g., polyethylene (PE), polypropylene (PP), and nylon fibers), and natural fibers (e.g., hemp, flax, and jute fibers) [20-22]. Recent research has shown that the use of hybrid fibers, rather than single type of fiber, is more effective for improving the spalling resistance of UHPC [23-25]. Hybrid fibers can provide a combination of different properties that can help to improve the overall performance of the UHPC, such as release of vapor pressure, high tensile strength, spalling resistance, and residual compressive strength. Numerous studies have been conducted regarding the utilization of a combination of steel and polymer fibers in UHPC, which is widely recognized for its ability to resist spalling [26]. But there have been relatively few studies on the use of hybrid steel and natural fibers in UHPC [27-30]. However, fiber-reinforced UHPC, whether single or hybrid fibers, is now commonly used for developing different types of structural members such as columns, beams, and slabs, to improve the spalling resistance.

The research area regarding the performance of hybrid fiber-reinforced UHPC under elevated temperature is still a new and hot topic. Therefore, this study aims to provide a state of art review of the influence of different fibers on the performance of UHPC under elevated temperature from material to structural level. The structure of this article comprises of: (a) the spalling behavior of fiber-reinforced UHPC (Section 2), (b) the residual mechanical properties, as well as the permeability of fiber-reinforced UHPC (Section 3), (c) the microstructure and chemical characterization of fiber-reinforced UHPC at elevated temperature (Section 4), (d) the spalling performance of full-scale structural member (Section 5), (e) and the summary and future perspective (Section 6).

2. Spalling behavior of fiber-reinforced UHPC

2.1 Spalling behaviors

Single fiber-reinforced UHPC: Different types of fibers have been investigated as effective reinforcements to prevent spalling of UHPC under elevated temperatures, as summarized in Table 1. Typically, three types of fibers are considered in UHPC: steel, polymer, and natural fibers. However, some studies [26, 31] have reported that steel fiber alone was insufficient to control spalling behavior, and explosive spalling was observed [32], as shown in Fig. 3. Conversely, other studies [18, 33] have reported that the addition of steel fibers alone did not

cause any spalling. Similar inconsistencies have been found when using different types of single-length polymer fibers in UHPC [34], as shown in Fig. 4. For example, it was proved that Low-Density Polyethylene (LLDPE), PP, and Polyamide (PA) fibers could improve the spalling resistance compared to Ultra-High Molecular Weight Polyethylene (UHMWPE) fiber. Zhang, et al. [20] reported that PE fiber alone did not provide sufficient resistance against spalling, even at a 1.5% content. However, single-length PP fiber showed better spalling results in UHPC at elevated temperatures with a 1.32% content [35]. For natural fibers, incorporating a single-length jute fiber was effective in reducing spalling of UHPC but required a higher fiber content (0.45%) [27]. Thus, the effectiveness of fiber reinforcements in preventing spalling of UHPC under elevated temperatures varies depending on the type and content of fibers used. Steel and polymer fibers have been extensively studied, and the results show inconsistencies regarding their ability to control spalling behavior. Natural fibers such as jute have shown promising results in reducing spalling, but a higher fiber content is required. Therefore, selecting an appropriate type and content of fibers is crucial in enhancing the spalling resistance of UHPC.

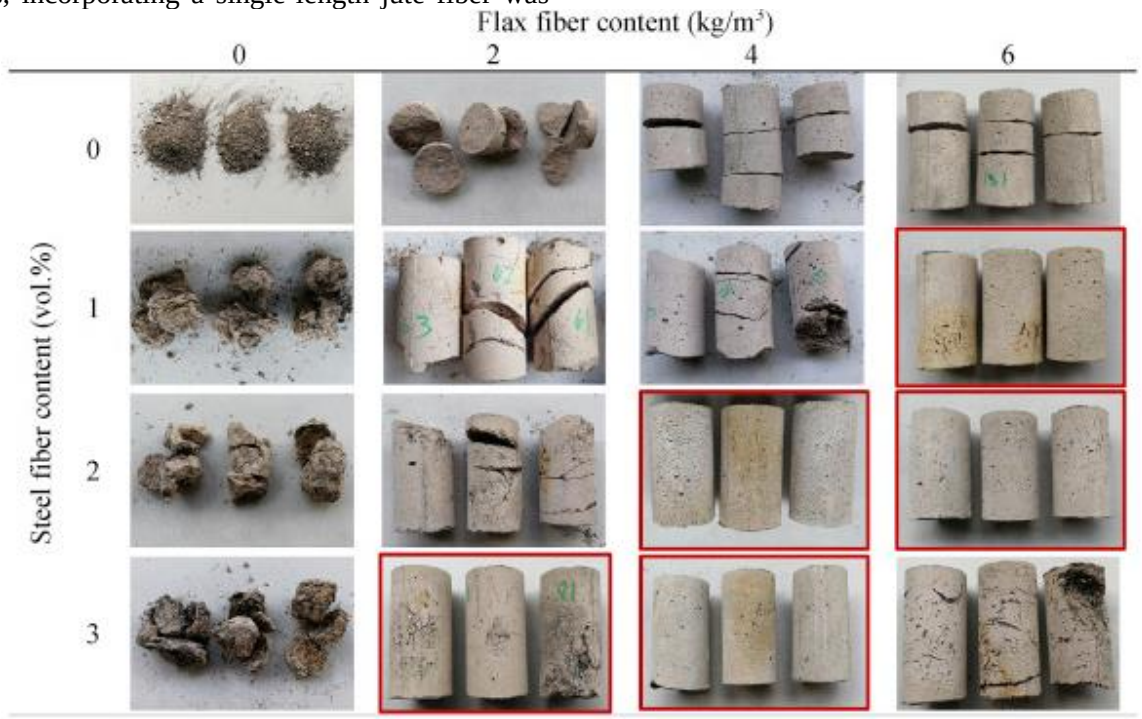

Fig. 3 – Spalling of UHPC with various steel fiber and flax fiber content [32]

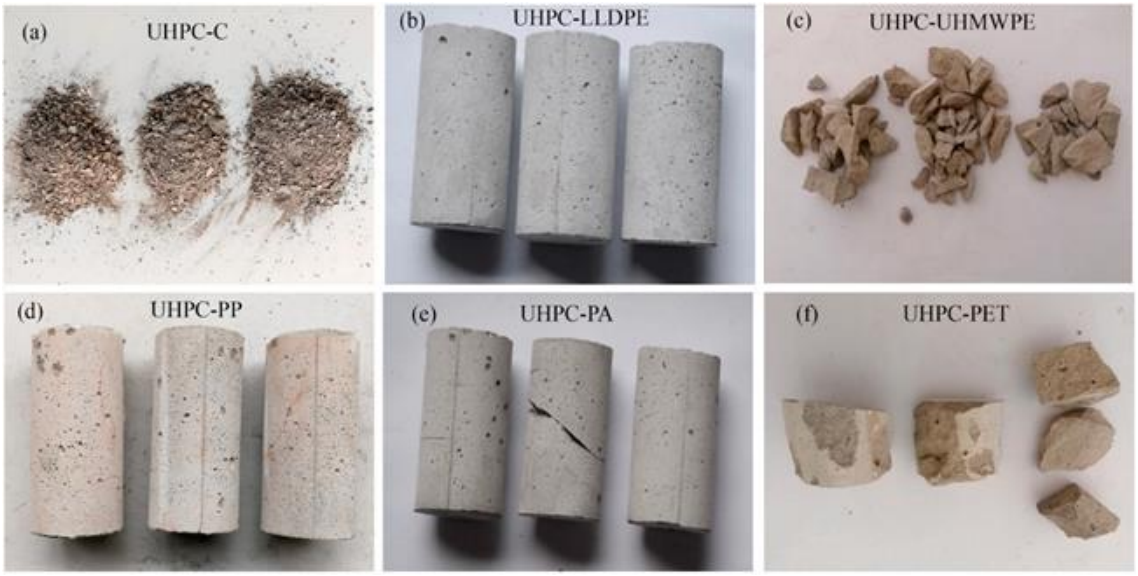

Fig. 4 – Spalling of UHPC [34]: (a) Control, (b) LLDPE fiber, (c) UHMWPE fiber, (d) PP fiber, (e) PA fiber, and (f) PET fiber

Hybrid fiber-reinforced UHPC: Another effective method for eliminating spalling or improving the spalling resistance of UHPC is through fiber hybridization. The use of hybrid fibers in UHPC has been found to be more effective in preventing spalling even at high temperatures of up to 1000°C as shown in Table 2. However, limited research is available on the use of hybrid polymer fibers. Zhang, et al. [20] reported that the hybrid use of 1%-1.2% PE fiber and 0.3%-0.5% PP fiber was effective for spalling resistance in UHPC. Typically, steel fibers are used for hybridization with polymer and natural fibers. Li, et al. [37] reported complete prevention of spalling with hybrid steel fibers (1%, 2%, and 3%) and PP fibers (4-6 kg/m^3). Similarly, the use of hybrid steel fibers with PP (0.4-0.6%) and Polyvinyl Alcohol (PVA) (0.3%-0.5%) has been found to be effective in preventing spalling [26]. The hybridization of steel fiber with PVA fiber demonstrated the best spalling resistance in UHPC, followed by PP and PE fibers. Furthermore, hybrid steel fibers with natural fibers, such as flax or sisal fibers, have been found to be effective in improving spalling resistance, as shown in Fig. 3. For example, complete prevention of spalling was achieved with a combination of 1% steel fibers and 0.45% flax fibers [32], and similarly the use of hybrid steel fibers (2%) with sisal fiber (0.6%) showed the greatest synergy effect in preventing spalling [30]. Thus, the use of fiber hybridization in UHPC has been found to be a promising method for improving spalling resistance. Steel fibers are commonly used for hybridization with polymer and natural fibers, and the results have shown that the selection of fiber types and contents greatly influences the spalling behavior of UHPC. Overall, fiber hybridization is a viable option for enhancing the spalling resistance of UHPC, and its potential should be explored further to develop more effective and efficient UHPC materials.

2.2 Spalling mechanisms

The working mechanisms of different fibers in UHPC may vary. Four mechanisms have been reported in the literature to explain how different fibers work in UHPC: vapor migration via pressure-induced tangential space [38], vapor migration via melting of polymer fibers [20], vapor migration via fibers/aggregates matrix interface [39], and vapor migration via fiber-matrix thermal expansion mismatch [34]. These mechanisms are described below.

Vapor migration via Pressure-induced tangential space (PITS): Fig. 5 shows a schematic view of the vapor migration though the PITS in PP fiber, jute fiber and steel fiber-reinforced UHPC. Khoury and Willoughby [38] first proposed this mechanism to explain the working mechanism of PP fiber. The polarity difference between PP fiber and matrix results in poor/weak interfacial adhesion. This weak bond region, called PITS, is susceptible to disruption by steam pressure at high temperatures. PITS can create a space for water vapor migration and offer a pressure release route even before fiber melting. Besides PP fiber, it has been reported that this mechanism also exists in steel fiber and jute fiber-reinforced UHPC. Ozawa et al. [29] stated that the carbonation of the straw-like structure of jute fiber results in PITS between the fiber and matrix interface. The release of vapor pressure through PITS of steel fiber was also stated in a previous study [40]. In summary, the PITS mechanism provides a viable explanation for the working mechanism of different fibers in UHPC, which can help to improve spalling performance. The mechanism of PITS is the same regardless of the type of fiber used.

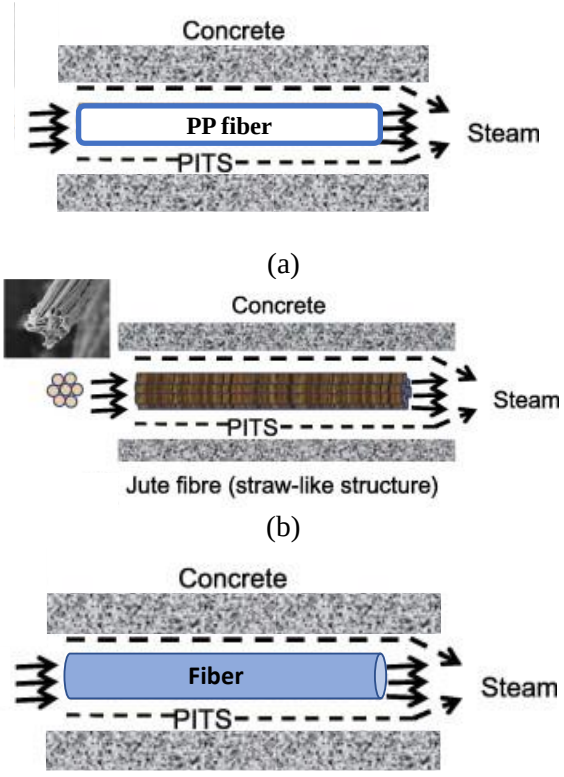

Fig. 5 – Pressure-induced tangential space (PITS): (a) PP fiber [41], (b) jute fiber [42], and (c) steel fiber [40]

Table 1. Single fiber-reinforced UHPC spalling behavior and other test parameters after exposure to elevated temperatures

Spalling behavior remarks	Heating rate (°C/min)	Target temperature (°C)	Curing method	Specimen size (mm)	Drying treatment before test	Constant heating time after target temperature	Cooling process	Reference UHPC Compressive strength	Reference
Steel fiber: 1%, spalling PP fiber: 0.15%, no spalling	ISO834	1050	Cured at a relative humidity of 98% at ambient temperature for 27 days	Cylinders Ø300 × 300 mm and Ø100 × 200 mm	-	2 hours	-	115–135 MPa	Du, et al. [31]
Steel fiber: 2%, spalling	1, 4, and 8°C/min	200, 400, 600, 800, 1000	Samples were submerged in a water tank at 90 °C for 1 day and then cured under standard curing until 28 days	Cube of 50 × 50 × 50	Kept in the oven at 90 °C for 24 h	2 hours	Natural cooling to ambient temperature	112-187 MPa	Liang, et al. [33]
Recycled PET fiber: 0.05%, spalling 0.10%, no spalling PP fiber: 0.05%, no spalling 0.10%, no spalling	5, 10°C/min	400, 600, 800	Moist curing for 91 days	Cube of 40 × 40 × 40	-	1 hour	Natural cooling to ambient temperature	122 MPa	Cai, et al. [36]
Jute fiber: 0.16%, spalling 0.33%, spalling 0.66%, no spalling	ISO834	200, 400, 600, 800	Samples were stored in lime-saturated water at ambient temperature for 28 days	Cylinder of Ø50 × 100	-	1 hour	Natural cooling to ambient temperature	118 MPa	Zhang, et al. [27]
PE fiber: 1.5%, spalling	ISO834	200, 400, 600, 800	Samples were stored in lime-saturated water at ambient temperature for 27 days	Cylinder of Ø50 × 100	Stored in the open air for another 3 months	1 hour	Natural cooling to ambient temperature	130 MPa	Zhang, et al. [20]

Spalling behavior remarks	Heating rate (°C/min)	Target temperature (°C)	Curing method	Specimen size (mm)	Drying treatment before test	Constant heating time after target temperature	Cooling process	Reference UHPC Compressive strength	Reference
Steel fiber: 1%, 2% and 3%, spalling PP fiber: 0.2%, 0.4% and 0.6%, spalling	ISO834	200	Samples were stored in lime-saturated water at ambient temperature for 27 days	Cylinder of Ø75 × 150	-	1 hour	Natural cooling to ambient temperature	141-147 MPa	Li, et al. [37]
Steel fiber: 1.5%, and 2.0%, spalling	ISO834	1050	Samples were submerged in a water tank at 90 °C for 2 days and then cured at ambient temperature until testing	Cylinder of Ø100 × 200	-	2 hours	Natural cooling to ambient temperature	207 MPa	Park, et al. [26]
LLDPE fiber: 0.3%, no spalling UHMWPE fiber: 0.3%, spalling PP fiber: 0.3%, no spalling PA fiber: 0.3%, no spalling PET fiber: 0.3%, spalling	ISO834	105, 150, 200, 300	Samples were stored in lime-saturated water at ambient temperature for 27 days	Cylinder of Ø50 × 100	-	1 hour	Natural cooling to ambient temperature	148 MPa	Zhang and Tan [34]
Steel fiber: 1%, 2% and 3%, spalling Flax fiber: 0.15%, 0.30% and 0.45%, spalling	ISO834	200, 400, 600, 800	Samples were stored in lime-saturated water at ambient temperature for 27 days	Cylinder of Ø50 × 100	-	1 hour	Natural cooling to ambient temperature	120-180 MPa	Zhang, et al. [32]

Spalling behavior remarks	Heating rate (°C/min)	Target temperature (°C)	Curing method	Specimen size (mm)	Drying treatment before test	Constant heating time after target temperature	Cooling process	Reference UHPC Compressive strength	Reference
Steel fiber: 1%, 1.5% and 2%, spalling	10 °C/min	800	Steam curing for 3 days at 90°C	Cylinder of Ø50 × 100	Pre-dried in the oven at 100 °C for 3 hours	2 hours	Natural cooling to ambient temperature	120-153 MPa	Ren, et al. [30]

Table 2. Hybrid fiber-reinforced UHPC spalling behavior and other test parameters after exposure to elevated temperature

Spalling behavior remarks	Heating rate (°C/min)	Target temperature (°C)	Curing method	Specimen size (mm)	Drying treatment before test	Constant heating time after target temperature	Cooling process	Reference UHPC Compressive strength	Reference
Steel + PP fiber: 1% steel + 2% PP fiber, no spalling	1, 4, and 8°C/min	200, 400, 600, 800, 1000	Samples were submerged in a water tank at 90 °C for 1 day and then cured under standard curing until 28 days	Cube of 50 × 50 × 50	Kept in the oven at 90 °C for 24 h	2 hours	Natural cooling to ambient temperature	112-187 MPa	Liang, et al. [33]
PE + PP fiber: 1.4% PE + 0.1% PP fiber, spalling 1.2% PE + 0.3% PP fiber, no spalling 1.0% PE + 0.5% PP fiber, no spalling	ISO834	200, 400, 600, 800	Samples were stored in lime-saturated water at ambient temperature for 27 days	Cylinder of Ø50 × 100	Stored in the open air for another 3 months	1 hour	Natural cooling to ambient temperature	130 MPa	Zhang, et al. [20]
Steel + PP fiber: 1% steel + 0.2% PP fiber, spalling 1% steel + 0.4% PP fiber, no spalling 1% steel + 0.6% PP fiber, no spalling	ISO834	200	Samples were stored in lime-saturated water at ambient	Cylinder of Ø75 × 150	-	1 hour	Natural cooling to ambient temperature	141-147 MPa	Li, et al. [37]

Spalling behavior remarks	Heating rate (°C/min)	Target temperature (°C)	Curing method	Specimen size (mm)	Drying treatment before test	Constant heating time after target temperature	Cooling process	Reference UHPC Compressive strength	Reference
2% steel + 0.2% PP fiber, spalling 2% steel + 0.4% PP fiber, no spalling 2% steel + 0.6% PP fiber, no spalling 3% steel + 0.2% PP fiber, spalling 3% steel + 0.4% PP fiber, no spalling 3% steel + 0.6% PP fiber, no spalling			temperature for 27 days						
Steel + PVA fiber: 1.5% steel + 0.1% PVA fiber, spalling 1.5% steel + 0.3% PVA fiber, no spalling 1.5% steel + 0.5% PVA fiber, no spalling Steel + PE fiber: 1.5% steel + 0.5% PE fiber, spalling Steel + PP fiber: 2% steel + 0.4% PP fiber, spalling 2% steel + 0.6% PP fiber, no spalling Steel + PP + Ny fiber: 2% steel + 0.1% PP + 0.1% Ny fiber, spalling 2% steel + 0.2% PP + 0.2% Ny fiber, no spalling 2% steel + 0.3% PP + 0.3% Ny fiber, no spalling	ISO834	1050	Samples were submerged in a water tank at 90 °C for 2 days and then cured at ambient temperature until testing	Cylinder of Ø100 × 200	-	2 hours	Natural cooling to ambient temperature	207 MPa	Park, et al. [26]

Spalling behavior remarks	Heating rate (°C/min)	Target temperature (°C)	Curing method	Specimen size (mm)	Drying treatment before test	Constant heating time after target temperature	Cooling process	Reference UHPC Compressive strength	Reference
Steel + Flax fiber: 1% steel + 0.15% Flax fiber, spalling 1% steel + 0.30% Flax fiber, spalling 1% steel + 0.45% Flax fiber, no spalling 2% steel + 0.15% Flax fiber, spalling 2% steel + 0.30% Flax fiber, no spalling 2% steel + 0.45% Flax fiber, no spalling 3% steel + 0.15% Flax fiber, no spalling 3% steel + 0.30% Flax fiber, no spalling 3% steel + 0.45% Flax fiber, spalling	ISO834	200, 400, 600, 800	Samples were stored in lime-saturated water at ambient temperature for 27 days	Cylinder of Ø50 × 100	-	1 hour	Natural cooling to ambient temperature	120-180 MPa	Zhang, et al. [32]
Steel + Sisal fiber: 1% steel + 0.3% Sisal fiber, spalling 1% steel + 0.6% Sisal fiber, no spalling 1% steel + 0.9% Sisal fiber, no spalling Steel + Sisal fiber: 1.5% steel + 0.3% Sisal fiber, spalling 1.5% steel + 0.6% Sisal fiber, no spalling 1.5% steel + 0.9% Sisal fiber, no spalling Steel + Sisal fiber:	10 °C/min	800	Steam curing for 3 days at 90°C	Cylinder of Ø50 × 100	Pre-dried in the oven at 100 °C for 3 hours	2 hours	Natural cooling to ambient temperature	120-153 MPa	Ren, et al. [30]

Spalling behavior remarks	Heating rate (°C/min)	Target temperature (°C)	Curing method	Specimen size (mm)	Drying treatment before test	Constant heating time after target temperature	Cooling process	Reference UHPC Compressive strength	Reference
2% steel + 0.3% Sisal fiber, no spalling									
2% steel + 0.6% Sisal fiber, no spalling									
2% steel + 0.9% Sisal fiber, no spalling									

Vapor migration via the channels formed by melting of polymer fibers: Fig. 6 and Table 2 illustrate the melting points of various types of fibers. Specifically, LLDPE, UHMWPE , PP, PA, and PET (polyethylene terephthalate) fibers exhibited melting points of 121.4°C, 144.3°C, 164.6°C, 257.8°C, and 250.5°C, respectively. When these polymer fibers undergo melting, empty channels can be created that allow for the release of trapped vapor pressure. These empty channels may also be connected by microcracks in UHPC, facilitating vapor migration. At room temperature, no significant cracking was observed in Fig. 7(a), but microcracks in the radial direction at the PP fiber interface were observed at 105°C, as shown in Fig. 7(b). The significant dimensional changes of PP fibers at 105°C (41 times greater than cement paste) resulted in radial microcracks [20], which could be widened with an increase in temperature or applied load. The interconnecting network of microcracks along the radial direction of PP fibers was observed at 150°C, as illustrated in Fig. 7(c). Furthermore, SEM images showed debonding of fibers from the matrix, and microcracks expanded in width and length at 170°C after melting PP fibers, as demonstrated in Fig. 7(d). Most PP fibers disappeared with further temperature increases to 200°C and 300°C, and the microcracks continued to widen in Fig. 7(e)-(f). This study emphasizes the importance of an interconnected microcracks network both before and after the melting point of fibers in enabling vapor migration via empty channels created by the melting of polymer fibers. Moreover, Bian, et al. [43] found that the melting of PP/PVA fibers was the primary reason for improved spalling resistance, and no significant contribution of steel fibers was observed. Thus, the findings suggest that the channels formed by the melting of polymer fibers can facilitate vapor migration, and an interconnected microcracks network is crucial for this process, which highlights the potential of hybridization with steel fiber to control cracking under elevated temperatures.

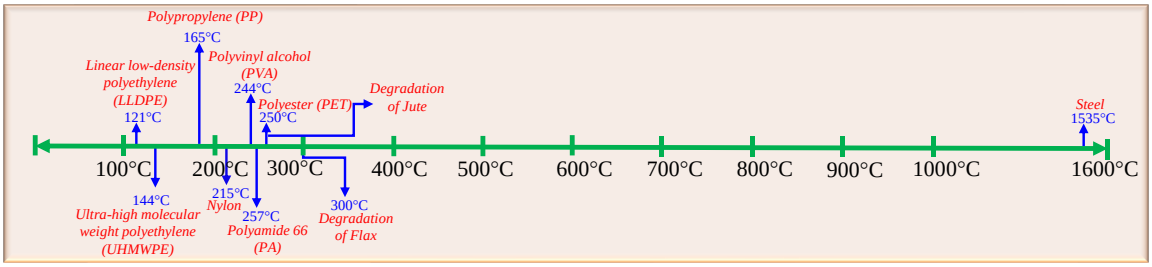

Fig. 6 – Fiber melting and degradation point in UHPC at elevated temperature

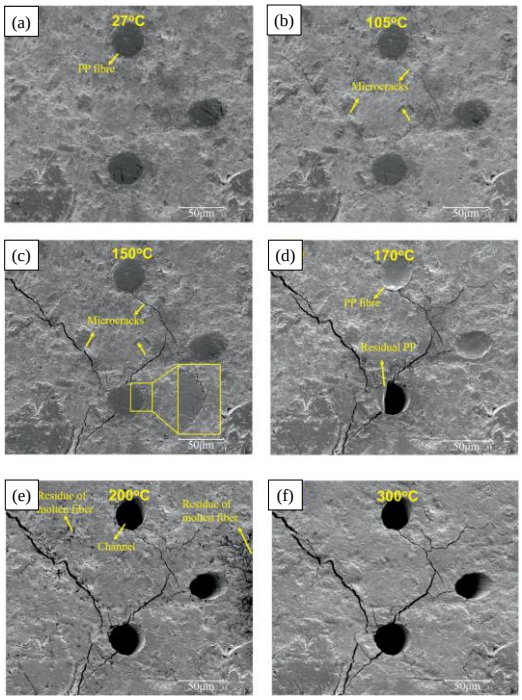

Fig. 7 – SEM image of PP fiber in UHPC [44]

Vapor migration via fibers and the matrix interface or aggregates and the matrix interface: Vapor migration can occur via fibers and the matrix interface or aggregates and the matrix interface in UHPC systems. In the absence of fibers, the porous ITZ between the aggregate and the matrix can create channels for vapor migration at elevated temperatures due to microcracks. However, Li, et al. [39] proposed a new mechanism for UHPC systems with larger aggregates (<5mm) and PP fibers to account for the effect of vapor migration. Specifically, microcracks are formed by the addition of larger aggregate and PP fibers, which initiate at high-stress areas and propagate along weak regions to release stress [45]. These microcracks provide connectivity between the empty pathways created by the PP fibers at elevated temperatures, as shown in Fig. 8(a). Fig. 8(b) illustrates the connectivity between microcracks, empty channels of PP fibers, and larger aggregates. It should be noted that the matrix cracks are produced by the combined effect of larger

aggregates and PP fibers. The higher vapor migration (its direction is shown using arrows) in UHPC systems with PP fibers and larger aggregates is due to the increased number of microcracks, larger volume fraction of microcracks, and greater surface area of matrix cracks at elevated temperatures. Overall, this proposed mechanism sheds light on the fundamental understanding of vapor migration in UHPC systems with larger aggregates and PP fibers, which can aid in the development of more spalling resistant UHPC.

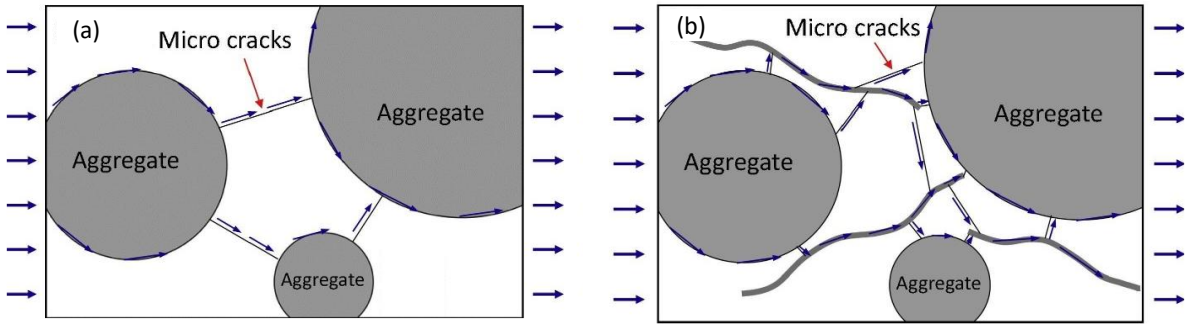

(a) (b)

Fig. 8 – Connection of ITZ in UHPC at elevated temperature [39]: (a) ITZ of micro cracks with ITZ of aggregates, and (b) PP fibers ITZ with micro cracks ITZ and aggregates ITZ

Vapor migration via the microcracks caused by the fiber-matrix thermal expansion mismatch: The thermal expansion of fibers is a critical parameter that affects the development of microcracks in UHPC systems [20, 34, 44]. Polymer fibers, including LLDPE, PP, and PA fibers, exhibit higher thermal strains than cement paste at elevated temperatures, as illustrated in Fig. 9 and Table 2. Zhang and Tan [34] proposed this mechanism to explain the behavior of polymer fibers. The thermal strain of polymer fibers was found to be 100 times higher than that of cement paste, which results in microcrack formation due to a higher thermal mismatch between the cement matrix and polymer fibers. PP fibers, in particular, can enhance vapor migration in UHPC systems via the development of microcracks resulting from their larger thermal expansion. As shown in Fig. 9 and Table 2, the thermal strain and coefficient of thermal expansion (CTE) of PE fibers were lower than those of PP fibers. The lower value of CTE for PE fibers can limit the formation of microcracks in the cement matrix, resulting in an inability to release buildup pore pressure. On the other hand, PP fibers had a higher CTE expansion and resulted in the creation of radial microcracks that increased the connectivity between empty channels, ultimately helping to release vapor pressure in UHPC systems at elevated temperatures. UHMWPE fiber had the smallest CTE among all polymer fibers, which means that it will not generate microcracks for vapor migration, as shown in Fig. 10. The use of hybrid steel and polymer fibers also improves vapor migration in UHPC systems [20]. However, steel fibers (shown in grey color) can also create microcracks along the radial direction due to thermal incompatibility between the UHPC matrix and fibers, as illustrated in Fig. 11. These microcracks developed around steel fibers can help to improve vapor migration by facilitating the connectivity of other cracks (e.g., those created by melted PP fibers). In summary, the thermal expansion behavior of fibers is a crucial parameter for understanding the development of microcracks and enhancing vapor migration in UHPC systems.

Table 2. Properties of fibers used in UHPC under elevated temperatures

Fiber type	Melting point (°C)	Coefficient of thermal expansion ($\times 10^{-3}$/°C)	Elastic modulus (GPa)	Density (kg/m^3)	Tensile strength (MPa)	Refs.
ST fiber	1540	-	303-550	7850	>3000	[43]
	1535	-	-	7850	-	[31]
PP fiber	154.8	-	1.4-2.2	910	300-750	[26]
	165	-	≥3.5	910	≥400	[33][46]
	170	-	-	910	-	[31]
	165	-	3.8	910	552	[20]
	164.6	3.6	-	-	-	[34]
	166.3	-	-	-	-	[36]
PET fiber	250.5	1.1	-	-	-	[34]
	243.6	-	-	-	-	[36]
PVA fiber	234.78	-	-	1300	1200	[26]
PE fiber	145	-	113	960	3250	[20]
LLDPE fiber	121.4	2.1	-	-	-	[34]
UHMWPE fiber	144.3	0.2	-	-	-	[34]
Ny fiber	215.8	-	3.9-4.9	1100	750-900	[26]
PA fiber	257.8	1.9	-	-	-	[34]
RPET fiber	245.8	-	-	-	-	[36]
Jute fiber	250*	-	-	-	-	[27]
Flax fiber	300*	-	-	1200-1400	-	[32]

Note: *Steel (ST) fiber, polypropylene (PP), polyvinyl alcohol (PVA), polyethylene (PE), linear low-density polyethylene (LLDPE), ultra-high molecular weight polyethylene (UHMWPE), nylon (Ny), polyamide 66 (PA), polyester (PET), recycled polyethylene terephthalate (PET).*

**Degradation starting point of natural fibers under elevated temperature.*

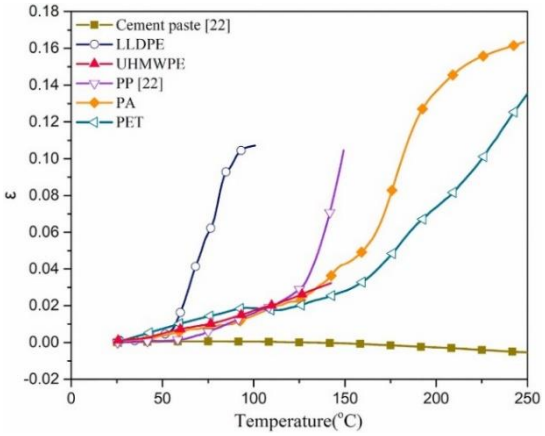

Fig. 9 – Thermal strain of different polymer fibers and cement paste [34]

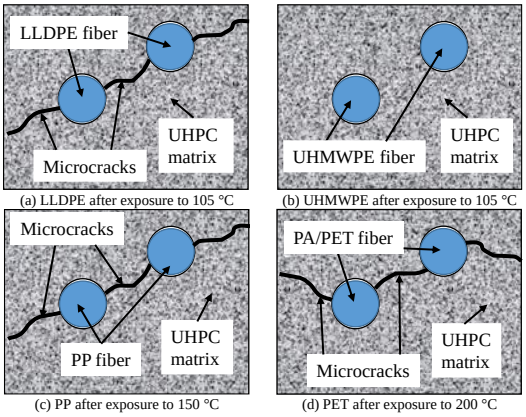

Fig. 10 – UHPC with various polymer fibers [34]

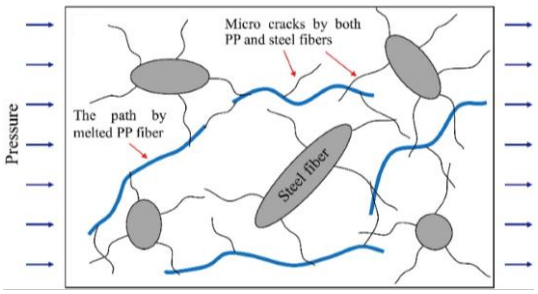

Fig. 11 – Hybrid steel and PP fibers connectivity via cracks [37]

3. Properties of single and hybrid fiber-reinforced UHPC

3.1 Residual mechanical strength after exposure to high temperatures

Residual mechanical strength refers to the strength of a material after it has been exposed to a high temperature and then cooled down to room temperature.

3.1.1 Compressive strength

Single fiber-reinforced UHPC: Steel fibers are commonly used in UHPC at elevated temperatures to improve the residual compressive strength by providing a bridging effect. Liang, et al. [33] only reported the residual compressive strength of 2% steel fiber-reinforced UHPC at 200°C because explosive spalling occurred after exposure to 400°C, and thus residual strength could not be measured. Similar conclusions were also reported by some other studies [26, 31, 32] using single-length steel fiber. On the contrary, some studies [18, 33] did not agree with such conclusions and reported the existence of residual compressive strength with single-length steel fiber in UHPC without spalling. In addition, it has been reported that other ingredients used in steel fiber-reinforced UHPC have a significant effect on the residual compressive strength after exposure to elevated temperatures. For instance, it has been reported that adding basalt coarse aggregate affects the residual compressive strength of steel fiber-reinforced UHPC. Fig. 12 compares the residual compressive strength of 1% steel fiber UHPC with and without basalt coarse aggregate. It was concluded that basalt coarse aggregate (5-16mm) having 1% steel fiber in UHPC demonstrated up to the residual 22% higher compressive strength than that of steel fiber UHPC without coarse aggregate.

On the other hand, single-length polymer fibers are also used to improve the residual compressive strength of UHPC after exposure to elevated temperatures. Xiong and Liew [47] reported the residual compressive strength of Polypropylene (PP) fiber in UHPC over 150 MPa with different PP fiber contents (0.1%, 0.25%, and 0.5%) after exposure to elevated temperatures. They found that the residual compressive strength of UHPC with 0.1% PP fiber was higher than that of PP fiber with 0.25% and 0.5% content at 600°C. Similarly, Du, et al. [31] recommended the use of PP fiber with a dosage equal to or higher than 0.15% by volume in UHPC for better residual compressive strength after exposure to elevated temperatures. However, polymer fibers do not contribute effectively to the residual compressive strength after melting, and a sudden decrease in compressive strength was observed after the melting of fibers [20]. Therefore, it has been proposed to hybridize PP fiber together with steel fiber to obtain better residual compressive strength, as discussed in the next section.

Nowadays, researchers also study the efficiency of single-length natural fibers in improving the residual compressive strength of UHPC after exposure to elevated temperatures. Zhang, et al. [27] investigated the influence of jute fiber on the residual compressive strength of UHPC after exposure to elevated temperatures, as shown in Fig. 13. Results showed that with a jute fiber dosage of 3 kg/m^3, the compressive strength of UHPC was similar to that of plain UHPC at all high temperatures tested. However, when the jute fiber dosage was increased to 5 kg/m^3 and 10 kg/m^3, a decrease in compressive strength was observed at ambient temperature. At high temperatures (>400°C), the decline in compressive strength became more pronounced with increasing fiber dosage, which was attributed to a combined degradation of both fiber and UHPC matrix.

The use of single fibers in UHPC after exposure to elevated temperatures has been a topic of research for many years, and steel fibers have been found to be efficient in improving the residual compressive strength of UHPC. However, the performance of fibers after exposure to elevated temperatures is influenced not only by the type and dosage of fibers but also by other ingredients used in UHPC, such as coarse aggregate. Moreover, the use of natural fibers in UHPC after exposure to elevated

temperatures is an area that requires further research.

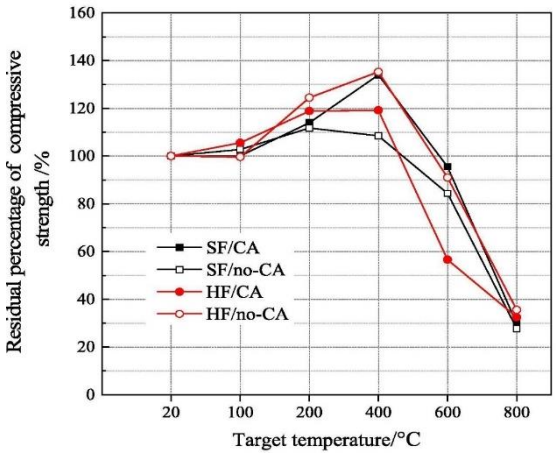

Fig. 12 – Residual compressive strength of UHPC with single steel and hybrid fibers [48]

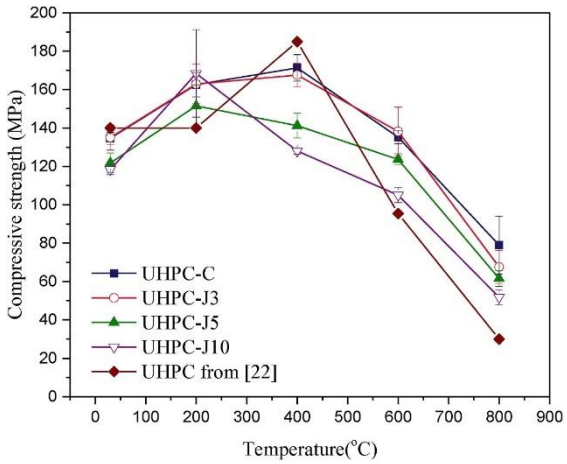

Fig. 13 – Residual compressive strength of fiber-reinforced UHPC with jute fiber [27]

Hybrid fiber-reinforced UHPC: The hybridization of polymer fibers with other polymer fibers is limited, as noted by Zhang, et al. [20], and may result in a sudden drop in residual strength after exposure to elevated temperatures due to melting of the fibers, as seen in Fig. 14. In contrast, hybridization of polymer fibers with steel fibers is commonly used in UHPC to retain higher compressive strength and avoid explosive spalling, ultimately offering better residual compressive strength. Liang, et al. [33] found that the residual compressive strength of UHPC with hybrid steel+PP fiber (1%ST+2%PP) was significantly higher than that of single PP fiber (2%) at 1000°C. Similarly, Park, et al. [26] studied hybridization of steel with PP, PVA, PE, and nylon (Ny) fibers and found that the hybrid use of steel with polymer fibers (PP, PVA, Ny) showed better residual compressive strength than the use of PE fiber alone. PVA fiber was more effective in improving the residual compressive strength than PP fiber. However, no clear trend was found with the hybrid use of steel, PP, and Ny fibers together. Fig. 15 shows the highest ratio (10.4%) of residual and original compressive strength for hybrid 2% steel with 0.3% PP + 0.3% Ny fiber. It should be noted that components like coarse aggregate used in preparing UHPC can also influence the mechanical strength of fiber-reinforced UHPC. Comparing the residual compressive strength of hybrid (1% steel+0.15% PP) fiber-reinforced UHPC with basalt coarse aggregate (UHPC-CA) having aggregate size range of 5-16 mm and without basalt coarse aggregate (UHPC-no-CA) at elevated temperature, it was found that using hybrid fibers with basalt coarse aggregate in UHPC presented a fast-decreasing trend at higher temperatures. The hybrid fiber without basalt coarse aggregate showed better residual compressive strength, as shown in Fig. 12. The hybrid of steel fiber with PP fiber having basalt coarse aggregate showed less residual compressive strength than that without coarse aggregate, likely due to the non-uniform fiber distribution caused by higher coarse aggregate content (0.30%). In general, steel fiber alone with coarse aggregate or hybrid steel and PP fibers without coarse aggregate offered better resistance of UHPC. Thus, the hybridization of polymer fibers with steel fibers is a common practice in UHPC to achieve better residual compressive strength after exposure to elevated temperatures and avoid explosive spalling. Hybridization of steel with other polymer fibers (PP, PVA, Ny) has also been found to improve residual compressive strength, except for PE fibers. However, the compressive strength of fiber-reinforced UHPC can also be influenced by components like coarse aggregate, and the optimal combination of fibers and aggregates should be carefully considered for achieving the desired performance.

Recently, researchers have shown interest in hybridizing natural fibers with steel fiber to improve the residual compressive strength of UHPC after exposure to elevated temperatures. Zhang, et al. [32] reported on the hybridization of different steel fiber contents (1%, 2%, and 3%) in UHPC with flax fiber contents (0.15%, 0.30%, and 0.45%) as shown in Fig. 16. This study found that steel fiber alone was not sufficient to provide residual compressive strength for UHPC (refer to Fig. 16(a)), but the addition of higher steel fiber

content bridged microcracks and sustained load. However, the use of hybrid steel with lower flax fiber content (0.15%) did not cause a significant reduction in strength, while higher flax fiber content (0.30% to 0.45%) resulted in up to a 15% reduction as shown in Fig. 16(b)-(d). This reduction in compressive strength could be suppressed by adding higher steel fiber content [49]. Incorporating steel fiber into UHPC can bridge microcracks and sustain load, and increasing steel fiber content reduces the space between fibers, thereby offering a bridging effect. However, hybridizing steel and flax fibers resulted in better residual compressive strength. The compressive strength of UHPC reduced at 400°C with hybrid steel-flax fiber, and the reduction rate increased sharply at 600°C due to flax fiber degradation, steel fiber-matrix bond reduction, and UHPC matrix degradation. Steel fiber starts to oxidize after exposure to 800°C, resulting in severe damage, and UHPC's compressive strength reduced to 55 MPa. Ren, et al. [30] studied the compressive strength of hybrid steel and sisal fiber in UHPC after exposure to temperatures of 800°C and reported that the optimal sisal fiber content in UHPC was 0.6%, with hybridization of 2% steel fiber content. Beyond this content, a negative effect on the residual strength of UHPC was observed due to the addition of higher sisal fiber content.

3.1.2 Tensile strength

Single fiber-reinforced UHPC: Limited research has been conducted on the residual tensile strength of single-fiber-reinforced UHPC after exposure to elevated temperatures. Park, et al. [26] investigated the effects of single-length steel fiber on the tensile strength of UHPC before and after exposure to an ISO 834 fire. They achieved tensile strengths of 16.3 MPa and 18.8 MPa under normal conditions with 1.5% and 2.0% steel fiber content, respectively. However, after exposure to an ISO 834 fire, no residual tensile strength was observed for the steel fiber-reinforced UHPC, as illustrated in Fig. 17. This is due to the decrease in bond strength of steel fiber after 400°C [50], and its oxidation at around 800°C [26], which has a negative effect.

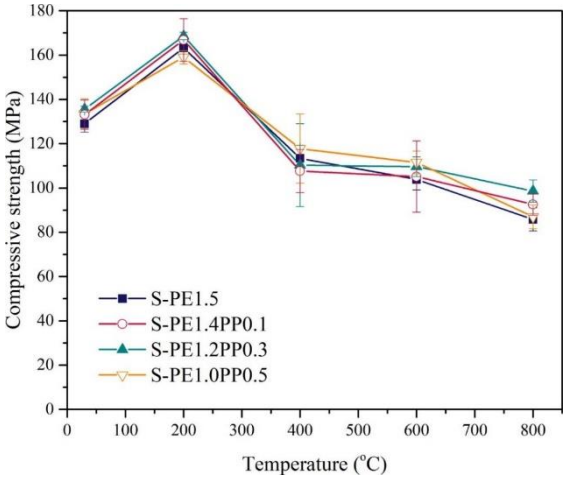

Fig. 14 – Residual compressive strength of hybrid polymer fibers [20]

Zhang, et al. [20] evaluated the effect of single-length PE fiber in UHPC after exposure to elevated temperatures, as illustrated in Fig. 17. They found that at 200°C, the tensile strength of UHPC with 1.5% PE fiber was reduced, and loss of strain-hardening behavior was observed due to the melting of fibers. As the temperature increased from 400°C to 800°C, there was a sudden decrease in tensile strength of UHPC reinforced with PP fibers due to the voids created by melted fibers, and the cracks caused by shrinkage in the UHPC matrix. Different types of single-length polymer fiber-reinforced UHPCs, such as PE-UHPC and PVA-UHPC, typically exhibit strain-hardening behavior under tensile loading at normal temperatures due to fiber bridging. However, at elevated temperatures, these fibers melt, resulting in the disappearance of strain-hardening characteristics.

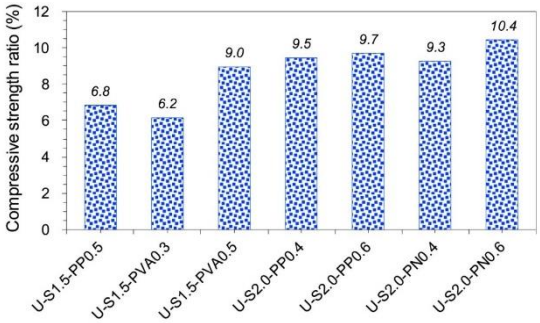

Fig. 15 – Residual compressive strength ratio of fiber-reinforced UHPC [26]

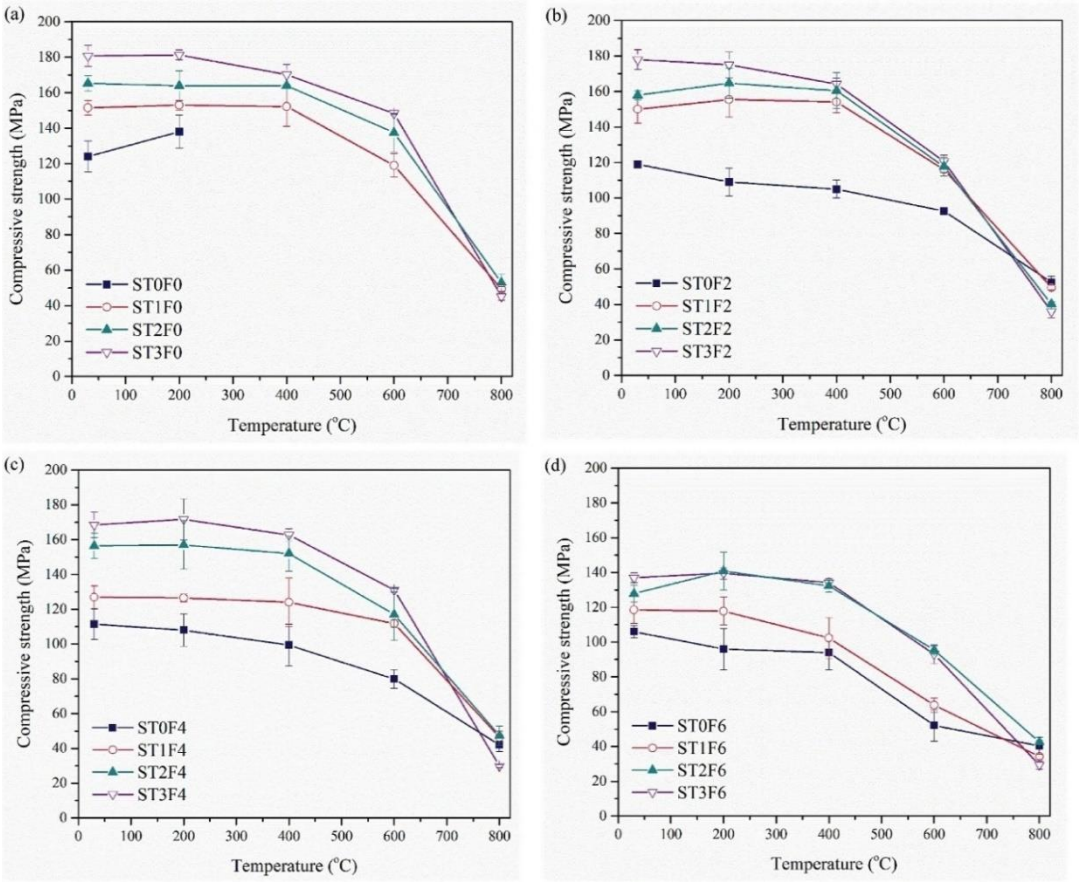

Fig. 16 – Residual compressive strength of steel-flax fibers reinforced UHPC [32]; (a) 0% flax fiber, (b) 0.15% flax fiber, (c) 0.30% flax fiber, and (d) 0.45% flax fiber

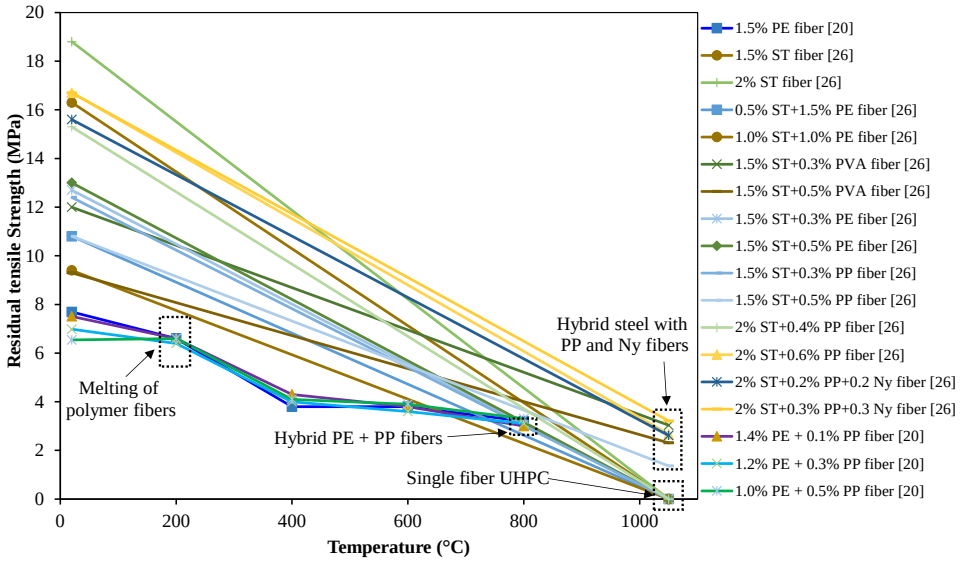

Fig. 17 – Residual tensile strength of UHPC with single and hybrid fibers

Hybrid fiber-reinforced UHPC: Fig. 17 shows the tensile behavior of UHPC with hybrid fiber after exposure to elevated temperatures. Zhang, et al. [20] evaluated the hybridization effect of PE and PP fiber in UHPC at elevated temperatures. At 200°C, the tensile strength of the hybrid PE and PP was slightly reduced due to fiber melting, which caused the loss of strain

hardening behavior. At 400°C, a higher reduction in tensile strength of the hybrid PE and PP was observed due to the creation of voids by melted fibers and cracks caused by shrinkage. With a further increase in temperature from 600°C to 800°C, the tensile strength was further reduced, and residual tensile strength of 25-38% was observed. However, only tensile strength was observed, and there was no strain hardening behavior because the fiber bridging effect vanished after the melting after exposure to high temperatures. This phenomenon is well-documented in the literature [51-53]. Park, et al. [26] also investigated the effects of hybrid fibers (i.e., steel, PVA, PE, PP, and Ny) on the tensile properties of UHPC after exposure to elevated temperature. In normal conditions, all hybrid fibers presented good results with strain hardening behavior. After exposure to an ISO 834 fire, residual tensile strength was observed only with a hybrid use of polymer and steel fibers, but this was only the case when steel fiber was more than 1.5% and polymer fibers (PVA and PP) were more than 0.5%. On the other hand, samples with steel and PE fibers did not present any residual strength, even with a higher PE fiber content of 1.5%. The hybrid of steel fiber was effective with PP and PVA fiber, but with a higher content of more than 0.5%. Another UHPC mix was also studied with three types of fiber hybridization, i.e., steel, PP, and nylon fiber. In this case, the hybrid of 2% steel fiber was adequate with a total polymer fiber content of 0.4% (0.2% PP+0.2% Ny) and 0.6% (0.3% PP+0.3% Ny). However, no residual tensile strength was found in the hybrid 2% steel fiber-reinforced UHPC with a total polymer fiber content of 0.2% (0.1% PP+0.1% Ny). Thus, the hybridization of 1.5-2.0% steel fiber content with PP, PVA, and Ny fiber (>0.4%) is efficient in achieving better residual tensile strength after exposure to elevated temperatures in UHPC. Overall, the tensile behavior of UHPC with hybrid fibers after exposure to elevated temperature has not been extensively studied in the literature. However, the use of PE fiber in the hybrid mix is not recommended as it does not provide any residual strength after exposure to high temperatures. Additionally, it has been observed that fiber melting at high temperatures causes a loss of strain hardening behavior in the hybrid UHPC, and the residual tensile strength is greatly reduced.

3.1.2 Flexural strength

Single fiber-reinforced UHPC: Studies on residual flexural strength in the literature are limited. Park, et al. [26] investigated the flexural strength of single-length steel fiber UHPC after exposure to elevated temperature. Under normal conditions, the highest flexural strength of 46.4 MPa was observed with 2.0% single steel fiber-reinforced UHPC. However, no residual flexural strength was found for single steel fiber-reinforced UHPC after exposure to fire. The reason is similar to what was mentioned earlier in the tensile strength section. Ren, et al. [30] examined the residual flexural strength and toughness of single-length sisal fiber-reinforced UHPC at 800°C, as shown in Fig. 18. The residual flexural strength of 12.4% and 10.6% was observed with 0.6% and 0.9% sisal fiber content, respectively. This indicates that sisal fibers can help reduce the damage to UHPC after exposure to 800°C. Based on the available literature, it can be concluded that residual flexural strength is generally not well-studied. Some studies have found that the addition of certain fibers, such as sisal fibers, can help reduce damage to UHPC at high temperatures. However, in general, the residual flexural strength of UHPC after exposure to fire appears to be significantly reduced. Further research is needed to better understand the residual flexural strength of UHPC and to develop strategies to improve its performance in high-temperature environments.

Hybrid fiber-reinforced UHPC: Park, et al. [26] also studied the steel fiber hybridization with PVA, PE, and nylon fiber for residual flexural strength according to the ISO standard. This study found that the residual flexural strength of hybrid steel with PE fiber could not be measured due to severe damage to the samples. The hybrid of 1.5% steel with PVA fiber (0.3% and 0.5%) enhanced the residual flexural strength more effectively than PP fiber alone (0.5%). The highest residual flexural strength was observed with the hybrid use of 2% steel, 0.3% PP, and 0.3% nylon fiber. Overall, the hybrid of steel with polymer fibers (PP, PVA, nylon) showed better residual flexural strength of UHPC except for PE fiber. Ren, et al. [30] also studied the hybrid steel fiber with sisal fiber in UHPC at a temperature of 800°C, as shown in Fig. 18. This study reported that a better residual flexural strength of 24.4% was observed with 2% steel fiber and 0.6% sisal fiber content, and beyond 0.6%, the strength declined. The residual flexural strength and toughness were greatly reduced due to the co-

deterioration of fibers and the UHPC matrix. From the available literature, it can be concluded that the hybridization of steel fibers with polymer fibers (such as PP, PVA, and nylon) generally enhances the residual flexural strength of UHPC, with the exception of PE fiber, which can result in severe damage to samples. Additionally, the addition of sisal fibers to UHPC can also improve its residual flexural strength at high temperatures. However, co-deterioration of fibers and the UHPC matrix can greatly reduce the residual flexural strength and toughness. Further research is needed to explore the potential of other fiber combinations and to develop strategies to mitigate the co-deterioration effect.

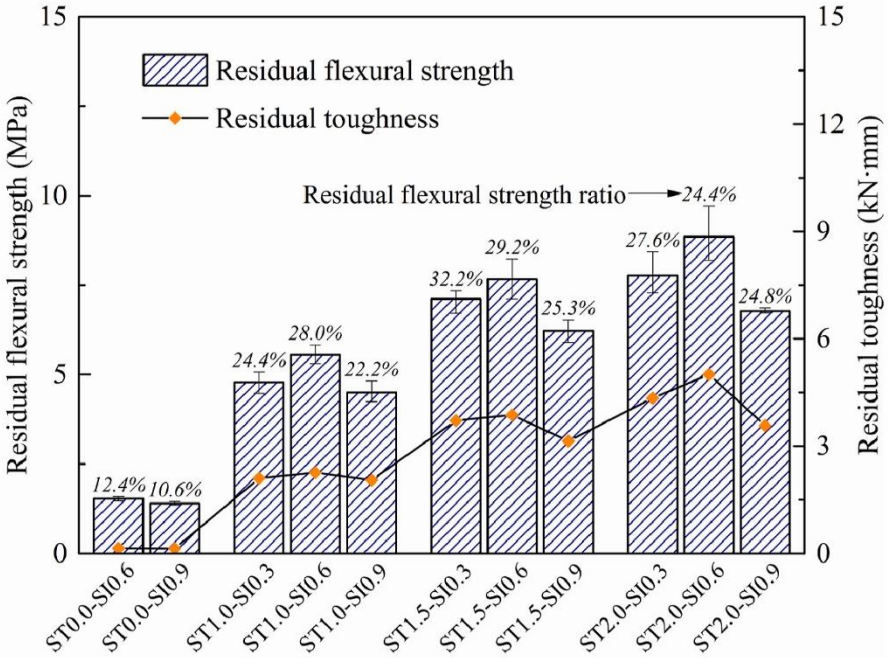

Fig. 18 – Residual flexural strength and toughness of fiber-reinforced UHPC [30]

3.2 Permeability

Single fiber-reinforced UHPC: The permeability of UHPC was mainly measured in the temperature range of 30°C to 300°C, as spalling is most noticeable within this range [39]. The permeability is highly related to the melting of polymer fibers, and most of the polymer fiber melting occurs before 300°C. Li, et al. [39] evaluated the permeability of steel fiber in UHPC at 200°C and found that the permeability of 2.5% steel fiber-reinforced UHPC was lower than that of UHPC without steel fibers. This is possibly due to the reduction of shrinkage-induced cracking by steel fiber bridging during the curing stage of UHPC specimens.

Li, et al. [39] also examined the permeability of PP fiber in UHPC. They reported that the single-length PP fiber-reinforced UHPC showed higher permeability than that of single-length steel fiber due to the melting of PP fibers, resulting in higher permeability at 200°C. Li, et al. [39] further explored the permeability of PP fiber in UHPC with and without coarse aggregate at 200°C. They reported that the PP fiber (3 kg/m^3) with coarse aggregate in UHPC presented a higher permeability than that of PP fiber without coarse aggregate at elevated temperatures. The PP fibers and larger coarse aggregates have a synergistic effect, forming an interconnected micro-crack network by melting PP fiber and by thermal mismatch between the matrix and fiber/aggregate, resulting in increased permeability.

Zhang, et al. [27] described the permeability of UHPC with single-length natural fiber up to 300°C, as shown in Fig. 19. The permeability of jute fiber-reinforced UHPC increases with an increase in temperature from 100°C to 300°C. The higher dosage of single-length jute fiber (3.5-10 kg/m^3) with a length of 12 mm provides better spalling performance because of the fiber's percolation, resulting in increased permeability as fibers shrink with temperature. The single-length natural fibers in UHPC exhibited lower permeability at elevated temperatures than polymer (PP or PE) fibers in UHPC. This is because polymer fibers melt at elevated temperature and leave channels behind, while natural fiber (jute or flax) only degrades/shrinks

under high temperatures. Thus, the permeability of UHPC is influenced by various factors such as temperature, type and dosage of fibers, and the presence of coarse aggregate. Understanding the factors that influence permeability is crucial in designing UHPC that can resist spalling and prevent damage due to exposure to high temperatures.

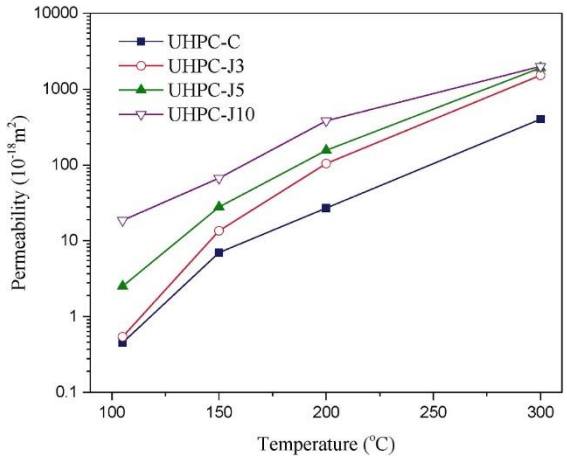

Fig. 19 – Permeability of UHPC with jute fibers [27]

Hybrid fiber-reinforced UHPC: Zhang, et al. [20] conducted an evaluation of the permeability of hybrid PP and PE fibers in UHPC at elevated temperatures, as depicted in Fig. 20. The permeability of the hybrid PP and PE fibers exceeded the measuring range of the permeability tester at 300°C. At 150°C, the hybrid of PE (1.0-1.2%) and PP fiber (0.3-0.5%) exhibited higher permeability than at 200°C, indicating that the PP fiber melted at higher temperatures, resulting in increased channels and higher permeability. However, the use of polymer fibers in UHPC beyond the optimum content leads to a significant increase in permeability (as shown in Fig. 20) and poor spalling performance at elevated temperatures up to 300°C.

Li, et al. [39] investigated the permeability of steel fiber with PP fiber in UHPC at 200°C. The study found that the permeability of 2.5% steel fiber-reinforced UHPC with PP fiber (3 kg/m^3) was higher than that of UHPC with single-length steel fibers. The increased permeability was due to the development of pathways/channels resulting from the melting of PP fiber at 200°C. In contrast, the hybrid of steel with PP fiber exhibited lower permeability than that of hybrid PP+PE fiber-reinforced UHPC. This is because unlike PP fiber steel fiber does not melt at lower temperatures and thus does not contribute significantly to increased permeability. However, at higher temperatures, radical cracks appear around steel fiber due to thermal mismatch, which ultimately improves the connectivity between cracks and enhances permeability. Thus, the polymer fibers contribute to increased permeability by melting and leaving channels behind at elevated temperatures.

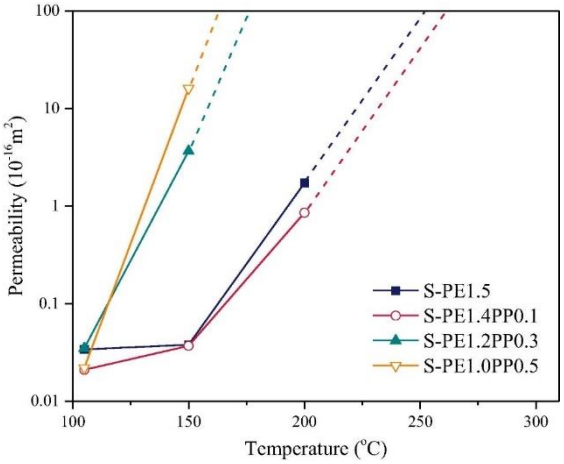

Fig. 20 – Permeability of UHPC hybrid polymer fibers [20]

Similarly, hybridization of natural fibers with steel fibers in UHPC at elevated temperatures has been studied. Zhang, et al. [32] found that the combination of flax and steel fibers increased permeability in UHPC at 200°C, with higher flax fiber content leading to higher permeability, as shown in Fig. 21. The hybridization of steel and flax fibers resulted in better spalling performance due to the combined effects of steel fibers creating microcracks and increasing connectivity, while natural fibers shrank at higher temperatures and increased permeability. The addition of steel fibers also mitigated thermal-induced cracking, reducing permeability. Ren, et al. [30] reported that increasing the steel fiber content (1%-3%) and sisal fiber content (0.3%-0.9%) in UHPC at 800°C increased permeability. However, too much sisal fiber content (0.9%) resulted in lower flowability and uneven distribution of fibers, leading to higher permeability. These findings are consistent with Zhang, et al. [32] conclusion about the effects of natural fibers on permeability in UHPC. In summary, the addition of natural fibers can increase permeability, while steel fibers can mitigate thermal-induced cracking by bridging effect and enhancing connectivity.

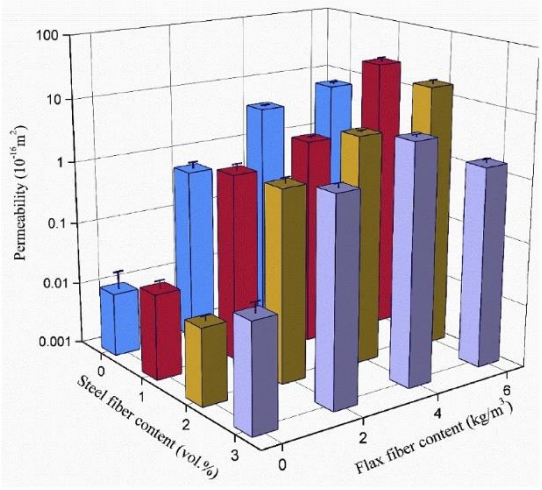

Fig. 21 – Permeability of UHPC hybrid steel and flax fibers [32]

4. Microstructural investigation and chemical characterization

4.1 SEM analysis

Single fiber-reinforced UHPC: The microstructure changes of fibers and matrix after being exposed to elevated temperature in fiber-reinforced UHPC were observed through SEM analysis. Cross-sectional images of UHPC with single-length steel fiber at ambient temperature and after exposure to 200°C are shown in Fig. 22(a) and Fig. 22(b), respectively. The steel fiber remained in the UHPC matrix after 200°C, but micro cracks in the radial direction were observed due to thermal incompatibility between the UHPC matrix and steel fiber, which confirmed the spalling mechanism (*fiber-matrix thermal expansion mismatch*) mentioned in section 2.2. Additionally, SEM images of single-length PP fiber in UHPC at ambient temperature and after exposure to 200°C are demonstrated in Fig. 22(c) and Fig. 22(d), respectively. The PP fiber disappeared after being exposed to 200°C, leaving an empty channel with a 5 μm wide micro crack in the radial direction. The shrinkage of the UHPC matrix due to the loss of humidity and the expansion of PP fiber resulted in tensile stress along the fiber-matrix interface in the radial direction, forming an interconnected network [37].

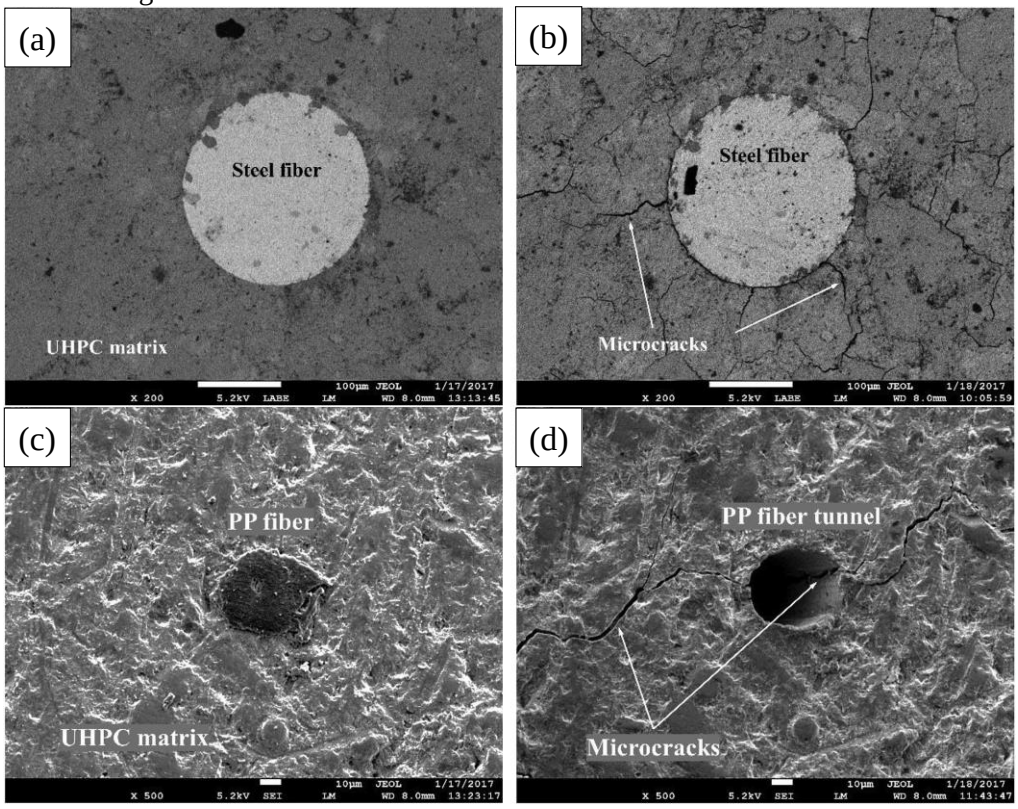

Fig. 22 – SEM images of steel and PP fiber in UHPC [37]: (a) steel fiber at ambient temperature, (b) steel fiber after exposure to 200°C, (c) PP fiber at ambient temperature, (b) PP fiber after exposure to 200°C,

Zhang and Tan [34] performed microstructure observation of single-length polymer fibers, including LLDPE, PP, PA, and PET fibers, in UHPC before the melting of fibers, as shown in Fig. 22(a)-(f). Microcracks were observed around the polymer fibers (LLDPE, PP, PA, and PET) in UHPC prior to the melting of fibers, as shown in the micrographs. This phenomenon was attributed to the high radial thermal expansion of polymer fibers, as discussed in Section 2.2. In addition, due to the lower thermal expansion of PET fibers, the microcracks created by PET fibers (Fig. 22(e)) were finer than those created by PA fibers (Fig. 22(d)). In contrast, fewer fine microcracks were found around UHMWPE fibers after exposure to 105°C due to its lower CTE (Fig. 22(b)). Fig. 22(f) depicts the SEM micrographs of UHPC-LLDPE after being subjected to 200°C, which clearly demonstrates that molten polymer fibers flowed out of the initial channels and remained on the surface of the samples. This supports the spalling mechanism reported in Section 2.2, where channels are formed by the melting of polymer fibers. In summary, the microstructure observation of polymer fibers in UHPC before the melting of fibers provides insights into the thermal mismatch between the fibers and matrix.

Zhang et al. [27, 32] conducted a microstructural analysis of single-length natural fibers (jute and flax fibers) reinforced UHPC before and after exposure to elevated temperatures, as depicted in Fig. 24. At ambient temperature, jute fibers exhibited poor bonding with the UHPC matrix, as seen in Fig. 24(a). This was due to the absorption of water by jute fibers during mixing and casting, resulting in swelling, which was later followed by deswelling during the enthalpy of hydration. Upon exposure to high temperature (up to 200°C), the jute fibers shrunk, leading to the separation of the fibers from the UHPC matrix at the interface (Fig. 24(b)). Similarly, shrinkage, debonding, and enlarged interfacial gaps of flax fiber at 200°C were observed in Fig. 24(c)-(d). These interfacial gaps can act as a pathway for releasing vapor pressure at elevated temperatures, which supports the spalling mechanism (*Pressure-induced tangential space (PITS)*) discussed in Section 2.2.

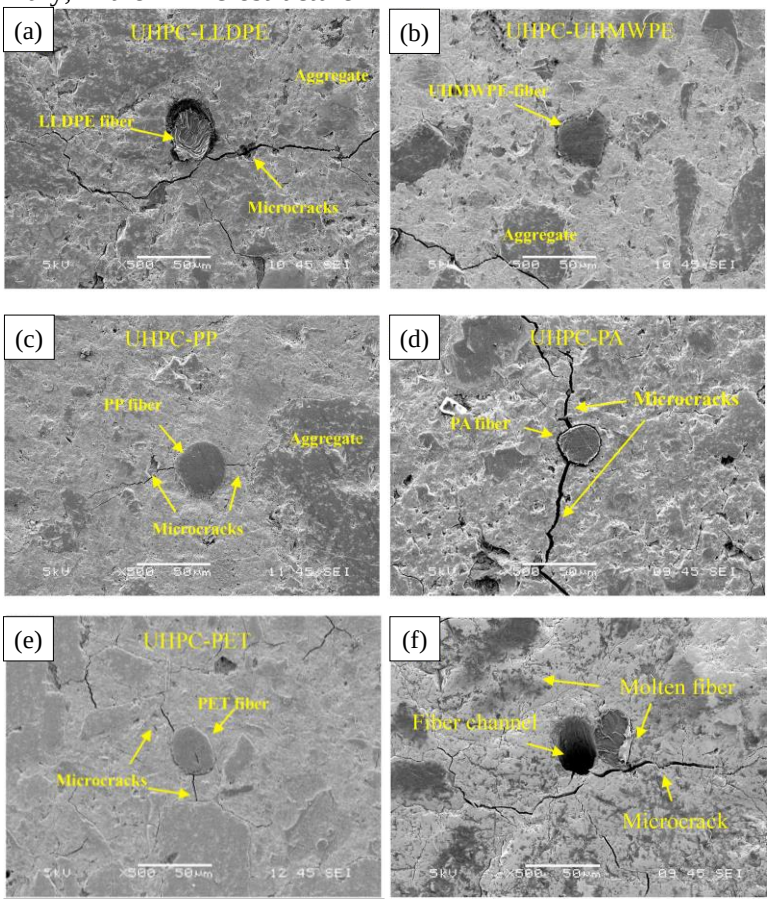

Fig. 23 – SEM images of UHPC [34]: (a) LLDPE at 105°C, (b) UHMWPE at 105°C, (c) PP at 150°C[34], (d) PA at 200°C, (e) PET at 200°C, (f) LLDPE at 200°C

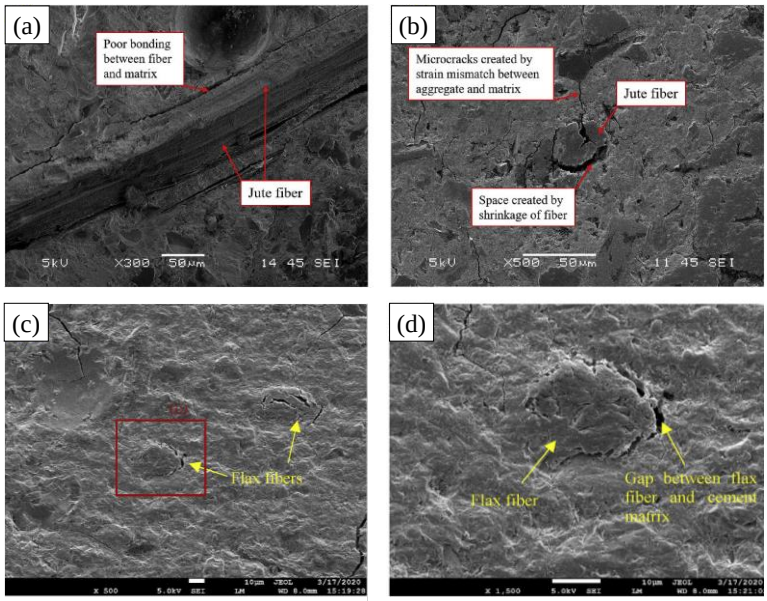

Fig. 24 – SEM images of natural fiber in UHPC: (a) jute fiber at ambient temperature [27], (b) jute fiber after exposure to 200°C [27], (c) flax fiber at ambient temperature [32], and (d) flax fiber after exposure to 200°C [32]

Hybrid fiber-reinforced UHPC: The microstructural analysis of hybrid steel-PP fibers was conducted to understand the synergistic mechanism of different fibers at elevated temperatures. The hybrid of steel fiber with PP fiber exhibited a synergetic effect, as shown in Fig. 25(a)-(b), with the melting of PP fiber and the formation of multiple microcracks for connectivity. The steel fibers did not melt, and no fiber tunnels were created, and microcracks were not well interconnected. Therefore, the melted channels created by PP fibers in UHPC helped improve the interconnectivity between cracks to release vapor pressure.

Similarly, the steel fiber also caused a limited number of radial microcracks due to thermal mismatch, and the cracks interconnectivity was limited to only steel fibers. Therefore, the hybrid use of steel with natural fibers, such as flax, in UHPC could connect with the interfacial gaps and enhance the interconnectivity at ambient temperature and after exposure to elevated temperature (refer to Fig. 26(a)-(b)). This enhanced interconnectivity results in increased permeability and provides pathways for the trapped moisture at elevated temperatures, as demonstrated in magnified images (see Fig. 26(c)-(d)). Thus, the hybrid use of steel with flax fiber resulted in the enhanced interconnectivity of cracks in UHPC to release vapor pressure under elevated temperature.

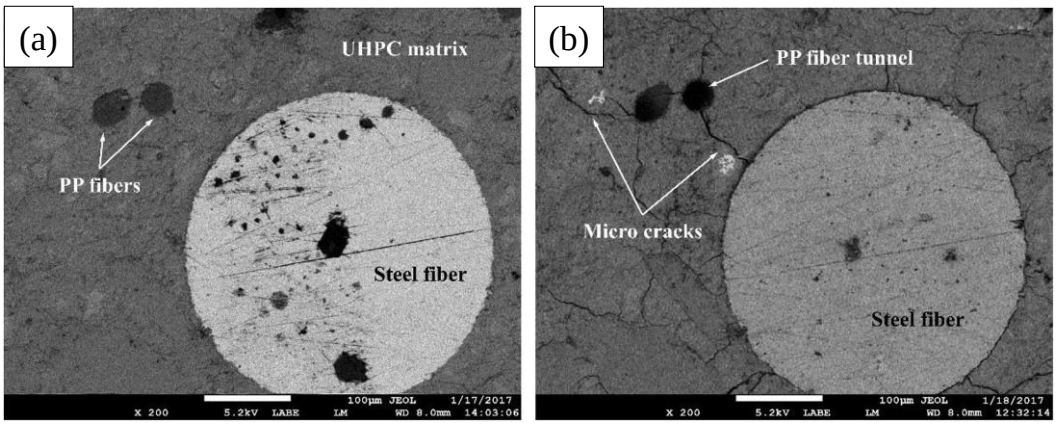

Fig. 25 – SEM images of hybrid PP and steel fiber in UHPC [37]: (a) hybrid steel-PP fiber at ambient temperature, and (b) hybrid steel-PP fiber after exposed to 200°C

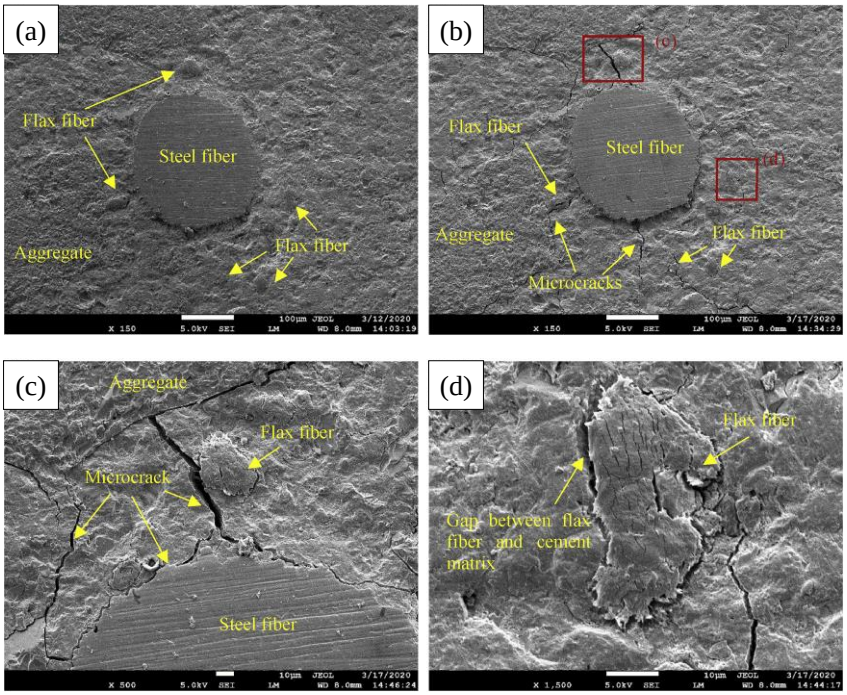

Fig. 26 – SEM images of hybrid steel and natural fiber in UHPC [32]: (a) steel-flax fiber at ambient temperature, (b) steel-flax after exposed to 200°C, (c) magnified image of steel fiber after exposed to 200°C, and (d) magnified image of flax fiber after exposed to 200°C

4.2 X-Ray Diffraction (XRD) analysis

Single fiber-reinforced UHPC: The phases identified in UHPC with 2.5% single-length steel fiber (refer to Fig. 27) were the same as those found in UHPC without steel fiber, except for the absence of rosenhahnite, which was only detected in the UHPC without fibers. The absence of rosenhahnite in steel fiber-reinforced UHPC could be attributed to the high reactivity of silica fume and its affinity for steel fibers, leading to the production of compact CSH [54, 55] structures around the steel fibers. The interface between the steel fibers and the binder tends to have more effective bonding. Since the intensity of the portlandite phase is low [56, 57], there is not enough free silica fume for pozzolanic activity in UHPC with steel fiber. At 200°C, the pattern of the quartz low-Dauphiné-twinned phase was altered, as shown in Fig. 27. This change in unit cell size for the quartz phase, together with pozzolanic reaction [27, 58], could explain the increase in compressive strength at 200°C; however, this increase was slightly less in the mixture and was not observed by XRD. The increased thermal damage within UHPC with steel fiber could be attributed to the gradual increase in the quartz unit cell and the expansion of steel fibers with increased temperature [59]. These changes could explain why explosive spalling of the UHPC mixture with some single steel fiber happened only in a few samples at temperatures of 300°C. Zhang, et al. [44] reported XRD results of UHPC with and without single-length PP fiber. No phase change was observed in UHPC with or without PP fiber until 250°C, as shown in Fig. 28(a)-(b). The peaks below 200°C were related to the evaporation of free water. The bounded water was lost around 250°C due to the dehydration of calcium silicate hydrate (CSH). In summary, XRD results indicate that the change in phases of UHPC was not attributed to fibers causing any chemical or physical changes.

Hybrid fiber-reinforced UHPC: The XRD spectra of UHPC with hybrid fiber (2.5% steel + 0.13% PP fiber) at room temperature and under elevated temperature were reported by Suescum-Morales, et al. [59]. Fig. 29 demonstrates that the phases for UHPC with hybrid fiber (2.5% steel + 0.13% PP fiber) were the same as those of UHPC without fibers at room temperature. The addition of steel fiber with a combination of PP fibers did not affect the diffractogram. This indicates that the fibers did not participate in the chemical reaction. Fig. 30 shows the XRD pattern at different temperatures from 100°C-300°C for hybrid steel-PP fibers in UHPC. As can be seen in the diffraction peaks obtained at 250°C (pink line) and 300°C (black line), the displacement

rises with increasing temperature. The phases discovered for UHPC with hybrid steel with PP fibers in Fig. 30 were the same as those identified in the single-length steel fiber-reinforced UHPC, excluding the formation of rosenhahnite, which was detected only in the UHPC without fibers. This indicates that the addition of PP fiber did not contribute to any chemical/physical change. A similar conclusion is also reported by Zhang, et al. [44]. Thus, the XRD spectra of UHPC with hybrid fiber showed that the phases present in the UHPC were not affected by the addition of fibers at room temperature, and under elevated temperatures.

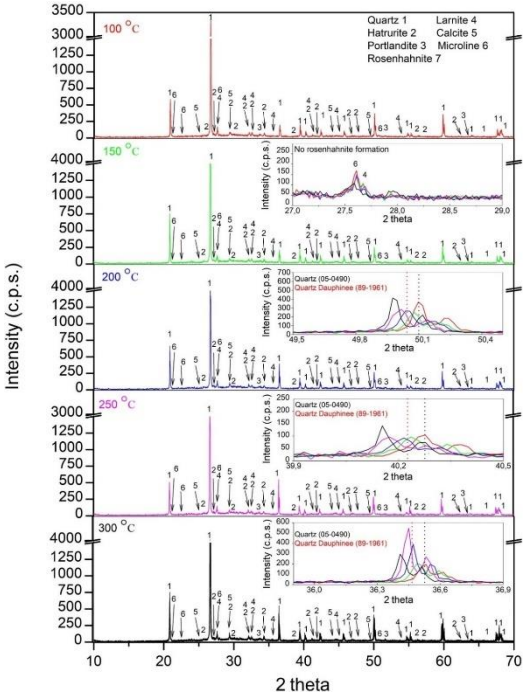

Fig. 27 – XRD spectra of UHPC with 2.5% steel fiber at elevated temperature [59]

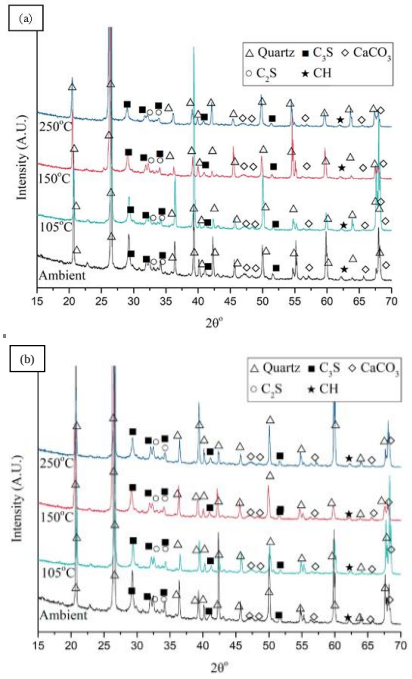

Fig. 28 – XRD spectra of UHPC [44]: (a) Without PP fiber; (b) 0.33% PP fiber

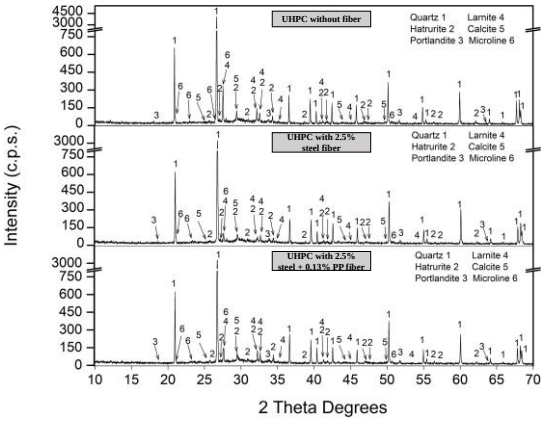

Fig. 29 – XRD spectra of UHPC with steel fiber and hybrid fibers at room temperature [59]

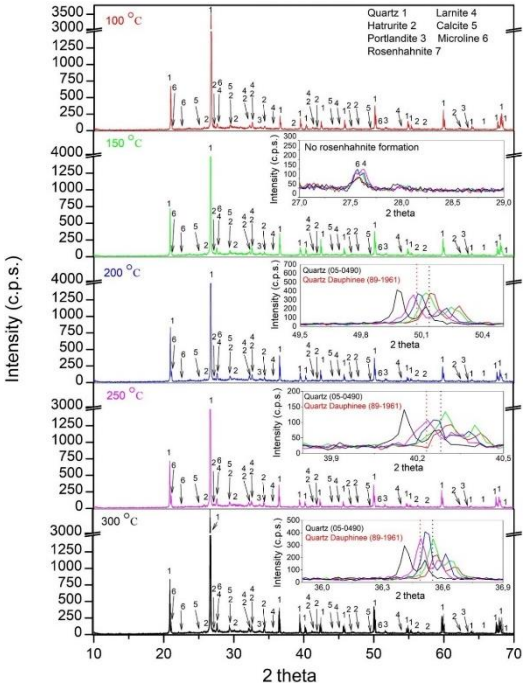

Fig. 30 – XRD spectra of UHPC with hybrid fibers (2.5% steel + 0.13% PP) at elevated temperature [59]

4.3 Mercury intrusion porosimetry (MIP) analysis

Single fiber-reinforced UHPC: MIP is a widely used technique for characterizing the distribution of pore sizes in fiber-reinforced UHPC materials. Zhang and Tan [34] compared the pore size distribution of UHPC with different polymer fibers at different temperatures using MIP analysis, as illustrated in Fig. 31. At ambient temperature (Fig. 31(a)), most of the pores in UHPC were below 0.04 μm. A peak could be found around 0.01 μm in the pore size distribution curve of each fiber-reinforced UHPC. The volumes of pores between 0.1 and 10 μm were similar in different mixes. At 105 °C (Fig. 31(b)), in UHPC-LLDPE, the volume of pores (size range: 0.1 to 10 μm) increased significantly due to the microcracks created by the thermal expansion of LLDPE fibers at this temperature. In contrast, UHPC-UHMWPE did not show any considerable increase in pore diameter at 105 °C. The pore size distribution of UHPC-UHMWPE samples in this range was similar to that in UHPC without fiber because UHMWPE fibers did not result in the formation of microcracks due to their low thermal expansion. At 150 °C (Fig. 31(c)), the volume of pores (size range: 0.1 to 10 μm) in UHPC-PP was much greater than that of plain UHPC, attributed to the formation of microcracks created by the thermal expansion of PP fibers. At 200 °C (Fig. 31(d)), an increase in the volume of pores (size range: 0.1 to 10 μm) was also found in UHPC-PA and UHPC-PET, compared to UHPC without fibers, attributed to the formation of microcracks created by the thermal expansion of PA and PET fibers. Additionally, in Fig. 31(d), the peaks at around 30 μm (approximately corresponding to fiber diameters) indicated the formation of empty channels due to the melting of fibers (including LLDPE, UHMWPE, and PP fiber) before 200 °C. Thus, the pore size distribution in UHPC varied depending on the type of polymer fiber used and the temperature, with some fibers leading to the formation of microcracks and empty channels at elevated temperatures.

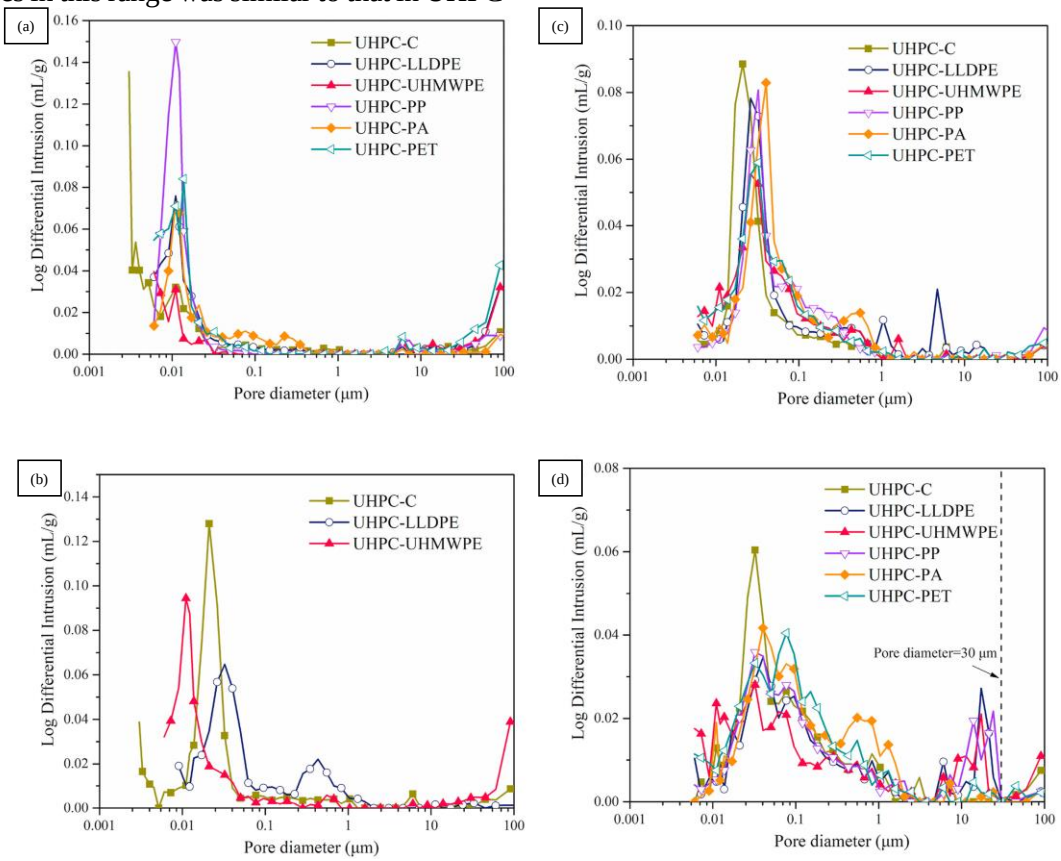

Fig. 31 – Pore size distribution of UHPC with polymer fiber [34]: (a) ambient temperature; (b) 105°C; (c) 150°C; and (d) 200°C

Hybrid fiber-reinforced UHPC: Fig. 32 depicts the effect of fire exposure on hybrid fiber-reinforced UHPC, showing that melting of PP fibers can cause an increase in porosity. Figure 32(a) compares the pore size distributions of hybrid fiber-reinforced UHPC (1.5% steel fiber + 0.5% PP fiber) before and after exposure to ISO fire using MIP analysis. It was found that the addition of PP fibers significantly increased the cumulative porosity of the sample after fire exposure due to melting of PP fibers and the formation of microcracks. The diameter of the PP fibers being 21μm, the porosity after melting of PP fibers increased significantly towards the pore sizes diameter ranging from 10-30μm. Park, et al. [26] also compared the cumulative porosity versus pore size responses of two hybrid UHPCs (1.5% steel fiber + 0.5% PP fiber vs 1.5% steel fiber + 0.3% PVA fiber) as shown in Fig. 32(b). However, the cumulative porosity versus pore size responses of the specimens of both hybrid fiber UHPCs were quite similar to each other. Due to the different diameters of PVA and PP fibers (15μm and 21μm, respectively), the points at which the porosity increased by melting the fibers were inconsistent: the PVA-fiber specimen provided an increase of porosity at a smaller pore size of around 10μm than the counterpart with PP fibers. However, below the pore size of 5μm (within which range the pores were caused due to the formation of microcracks in the matrix), their porosity and pore size distributions were quite similar, indicating that the matrix damage from the fire was also very similar.

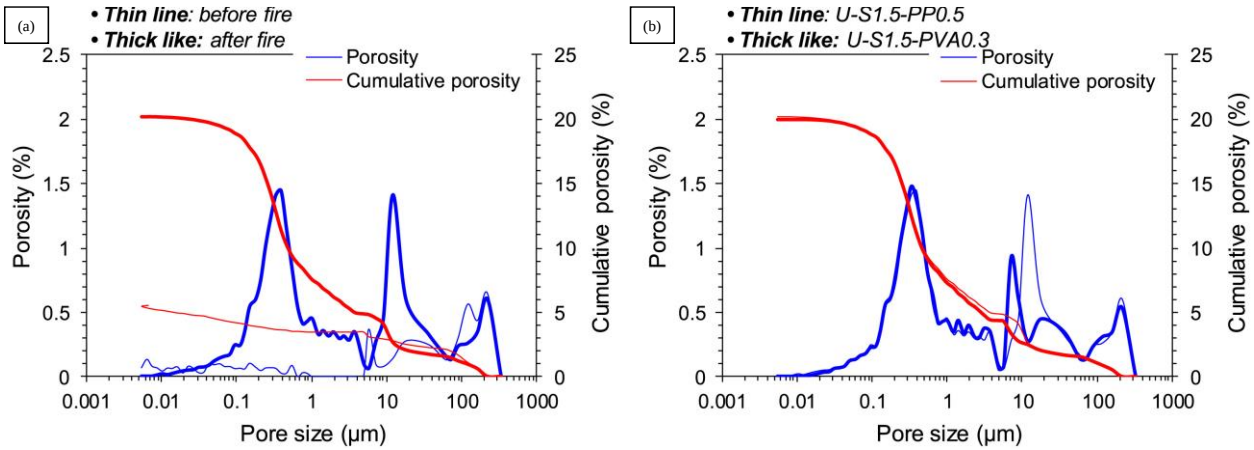

Fig. 32 – Pore size distributions of hybrid fibers in UHPC [26]: (a) 1.5% steel+0.5%PP fiber; (b) 1.5% steel+0.3%PVA fiber

5. Fiber-reinforced UHPC structural members under fire

Fiber-reinforced UHPC has been widely used to strengthen structural members at ambient temperature [60]. Full-scale experimental testing of UHPC structural members (such as columns and beams) with fibers at elevated temperatures has also been carried out. However, there still is a lack of codes/standards for testing full-scale structural members due to the special requirements for heating specimens to high temperatures. The full-scale testing of columns and beams reported in the literature is discussed below.

5.1 Column

Single fiber-reinforced UHPC: Table 3 presents the details of single fiber-reinforced UHPC structural members at elevated temperatures. Li, et al. [61] assessed the behavior of UHPC column members under elevated temperatures following ISO standards for testing and studied the influence of UHPC strength and fiber addition. UHPC without fibers was found to be vulnerable to explosive spalling, but spalling was not observed in UHPC block specimens (200 x 200 x 400 mm) under unstressed conditions with the addition of PP fibers. However, spalling was observed in UHPC with PP fibers under axial load, even though the PP fiber dosage (3 kg/m^3) was greater than the suggested dosage (2 kg/m^3) in Eurocode 2 [62]. This clearly indicates that the loading condition can promote the spalling of fiber-reinforced UHPC.

Hybrid fiber-reinforced UHPC: Lee, et al. [22] evaluated the full-scale column behavior of UHPC with the addition of hybrid fibers (PP, nylon, and steel fibers) at high temperatures. Initially, small UHPC cylinders (100 x 200 mm)

were tested with hybrid fibers, and the spalling performance was evaluated. The addition of hybrid fibers was found to be more effective in preventing spalling in UHPC as compared to single-length fiber-reinforced UHPC. Then, two same full-scale hybrid fiber (PP, nylon, and steel fibers) reinforced UHPC columns with compressive strength of 200 MPa were constructed and tested under high temperatures using ISO standard fire. Fig. 33(a) demonstrates that both columns had minor spalling with a maximum depth of spalling of 10 mm on a small part of one side. Consequently, both columns passed the ASTM E 119 load capacity criterion, which defines that, if the column can sustain the applied loads after fire exposure, then the test is successful. Both columns met the Korean fire code's requirements in terms of temperature. According to the Korean code, the test is considered successful if the steel rebar's average temperature at four measured points is not more than 538°C, or the temperature at any of the observed points is not more than 649°C under 3 hours of fire exposure [22]. Li, et al. [61] also reported good spalling resistance of UHPC block specimens (200 x 200 x 400 mm) with the inclusion of hybrid steel and PP fiber due to their positive synergetic effect that helped to release trapped vapor pressure, as explained in section 2 above. It's worth noting that water vapor was continuously discharged to the floor of the testing lab from the furnace during the test. The addition of steel fiber prevented spalling of UHPC in the deeper region of the cross-section and also helped in preventing the exposure of reinforcement to elevated temperatures. Additionally, load eccentricity is another governing parameter for spalling behavior. Surface spalling was observed in UHPC with hybrid fibers on the compressive side of an eccentrically loaded column, while there was no spalling on the tension side because cracking on the tension side resulted in reduced vapor pressure (refer to Fig. 33(b)). Du, et al. [31] reported on the behavior of ultra-high-strength concrete (UHSC) columns with the addition of PP and steel fibers. Fig. 33(c) shows that two different column lengths were considered. No spalling was observed with the addition of hybrid steel and PP fiber in the large-scale column subjected to the applied load, even with a lower dosage (1.365 kg/m^3) of PP fiber than the recommended dosage in Eurocode 2 [62]. Buckling was found to be the dominant failure mode for all specimens, and the addition of 1% steel fiber resulted in improved ductility. The spalling/cracking behavior was not affected by the increased specimen size of the UHSC column. The addition of steel fiber reduced the intensity of explosive spalling and prevented spalling. Therefore, 1% steel fibers with 1.365 kg/m^3 were effective for casting large-scale UHSC columns in terms of workability and spalling prevention. However, further in-depth analysis is needed for the study of fiber-reinforced UHPC columns considering different types of hybrid fiber, and various strengthening and repair methods, especially for columns already damaged after being exposed to fire.

5.2 Beams

Single fiber-reinforced UHPC: Banerji, et al. [63] evaluated the structural behavior and spalling performance of steel fiber-reinforced UHPC beams under elevated temperatures. The spalling behavior with a schematic representation is shown in Fig. 34, and severe spalling was observed with single-length steel fiber having a content of 1.5%. It is worth mentioning that spalling in most beams was observed on the upper side (compression zone), and a minor level of scaling/spalling was indicated on the bottom side (tension zone) of the beam. The bottom layer of the beam experiences tensile cracking prematurely resulting in low pore pressure due to the escape of vapor pressure. The escape of vapor pressure was different in different parts of the beam along the cross-section because of crack patterns caused by bending moment variation at different levels under applied loading. It was concluded that spalling depends on the time of occurrence, nature, and location, i.e., explosive spalling is observed in the compression zone at the early stage, while non-explosive spalling is observed in the tension zone at the intermediate and later stages. Vapor pressure cannot escape from the fiber-reinforced UHPC beam at the top compression zone due to lower permeability resulting from the absence of tensile cracking. Kahanji, et al. [64] also assessed the spalling behavior of beams under elevated temperatures. They found that a 2% steel fiber fiber-reinforced UHPC beam (Fig. 35(a)) is more susceptible to spalling than a 4% steel fiber fiber-reinforced UHPC beam, as shown in Fig. 35(b). The addition of more steel fiber provides higher tensile strength that resists pore pressure and ultimately reduces spalling.

Hybrid fiber-reinforced UHPC: Banerji, et al. [63] found that UHPC beams reinforced with

a combination of steel and PP fibers exhibited lower spalling (5.4% by weight) compared to beams reinforced solely with single-length steel fibers (7.5% by weight). The reduced spalling in the hybrid fibers reinforced beams was attributed to the melting of PP fibers, which created voids that improved crack connectivity, particularly in the tensile zone, leading to the release of vapor pressure. Kahanji, et al. [64] reported no spalling in the fiber-reinforced UHPC beam reinforced with both steel and PP fibers, as shown in Fig. 35(c), suggesting the effectiveness of PP fibers in preventing spalling in UHPC beams. Thus, the addition of PP fibers to steel fiber-reinforced UHPC can effectively reduce the spalling behavior of UHPC beams under elevated temperatures, thereby enhancing their structural performance.

6. Summary and future outlook

6.1 Conclusions and summary

This article provides a comprehensive understanding of recent advances in the fire performance of fiber-reinforced UHPC using single-length and hybrid fibers. It covers the spalling behavior, spalling mechanism, mechanical properties, microstructure characteristics, and structural member performance of fiber-reinforced UHPC after exposure to elevated temperatures, as reported in the literature. The following are the key findings from the review:

- Fire-induced spalling is one of the major concerns in UHPC, which can be caused by the buildup of pore pressure, thermal-induced stress, and a combination of both. At different temperatures, spalling can be classified as thermo-hydral spalling, thermo-mechanical spalling, and thermo-chemical spalling, which are related to various stress sources.
- The addition of fibers can play an important role in preventing spalling, and four responsible mechanisms for different types of fiber have been reported in the literature. These mechanisms include vapor migration via Pressure-induced tangential space (PITS), vapor migration via channels formed by melting of polymer fibers, vapor migration via fibers/aggregates matrix interface, and vapor migration via microcracks caused by the fiber-matrix thermal expansion mismatch.
- The addition of hybrid steel and PP fibers to UHPC was found to significantly improve its residual compressive strength, while combining steel fibers with higher natural fiber content improved spalling resistance. UHPC with hybrid steel and polymer fibers also showed better tensile and flexural strength than UHPC with single steel fibers. However, it is important to note that as polymer fibers melt at elevated temperatures in UHPC, no strain hardening can be achieved after melting.
- UHPC with a hybrid of steel, polymer, and natural fibers has higher permeability than UHPC with a single fiber type, which improves spalling performance by releasing vapor pressure. Permeability can be influenced by factors such as fiber melting and coefficient of thermal expansion at elevated temperatures. Therefore, when selecting fibers to avoid spalling, mechanical strength and bonding properties of fibers should be considered along with permeability.
- SEM analysis indicates that steel fibers limit crack propagation and improve connectivity between empty channels/interfacial gaps in UHPC, while polymer and natural fibers create radial microcracks that facilitate vapor migration. Combining steel with polymer/natural fibers has a positive synergistic effect that improves spalling behavior, which cannot be achieved with a single-length fiber in UHPC.
- XRD analysis indicates that the addition of steel fiber alone or in combination with other fibers did not affect the diffractogram, suggesting that the fibers did not participate in the chemical reaction.
- MIP analysis shows that UHPC with PP fiber has a significantly greater volume of pore diameter than UHPC without fibers, due to microcracks created by PP fiber thermal expansion, leading to higher permeability. However, empty channels created by melting polymer fibers after a certain point did not substantially increase permeability or affect spalling resistance. The cumulative porosity versus pore size responses were the same for hybrid steel and polymer fibers, despite different types of polymer fibers being used.

Table 3. Single and hybrid fiber-reinforced UHPC structural members at elevated temperature

Specimen type / size (mm)	**Heating rate (°C/min)**	**Target temperature (°C)**	**Total heating time**	**Fiber content and type**	**Drying treatment before test**	**Cooling process after test**	**Ref.**
Column / 200 × 2900	ISO834	1050	2 hours	Single (0.33% PP, 2.5% Steel) and Hybrid fibers (2.5% Steel + 0.33 % PP, 1% Steel + 0.22 % PP) Steel fiber = 13, 35 mm PP fiber = 12 mm	Ambient temperature	Cooled down to below 50°C in the furnace	[61]
Column / 500 × 3428	ISO834	1050	3 hours	Hybrid fibers (0.5% Steel + 0.2 % PP + 0.2% Nylon) Steel fiber = 25 mm PP fiber = 12 mm Nylon fiber = 12 mm	Laboratory condition	Natural air cooling	[22]
Column / 300 × 1400 Column / 300 × 2500	ISO834	1050	2 hours	Hybrid fibers (0.5% Steel + 0.15% PP) Steel fiber = 16 mm PP fiber = 14 mm	-	-	[31]
Beam / 180 × 270 × 4000	ASTM E119	900	1.5 hours	1.25% steel fibers, Hybrid fibers (1.5% Steel + 0.11% PP) Steel fiber = 13 mm PP fiber = 13 mm	-	Natural cooling	[63]
Beam / 100 × 200 × 2000	ISO834	900	1 hour	2% steel fibers, 4% steel fibers, Hybrid fibers (2% Steel + 0.44% PP) Steel fiber = 13 mm PP fiber = 12 mm	-	-	[64]
Beam / 250 × 350 × 3700 (shear) Beam / 250 × 350 × 6500 (flexural)	ISO834	1050	2.5 hours	2% steel fibers, Hybrid fibers (2% Steel + 0.2% PP) Steel fiber = 13 mm PP fiber = 12 mm	Samples were stored in laboratory environment for 90 days	-	[65]

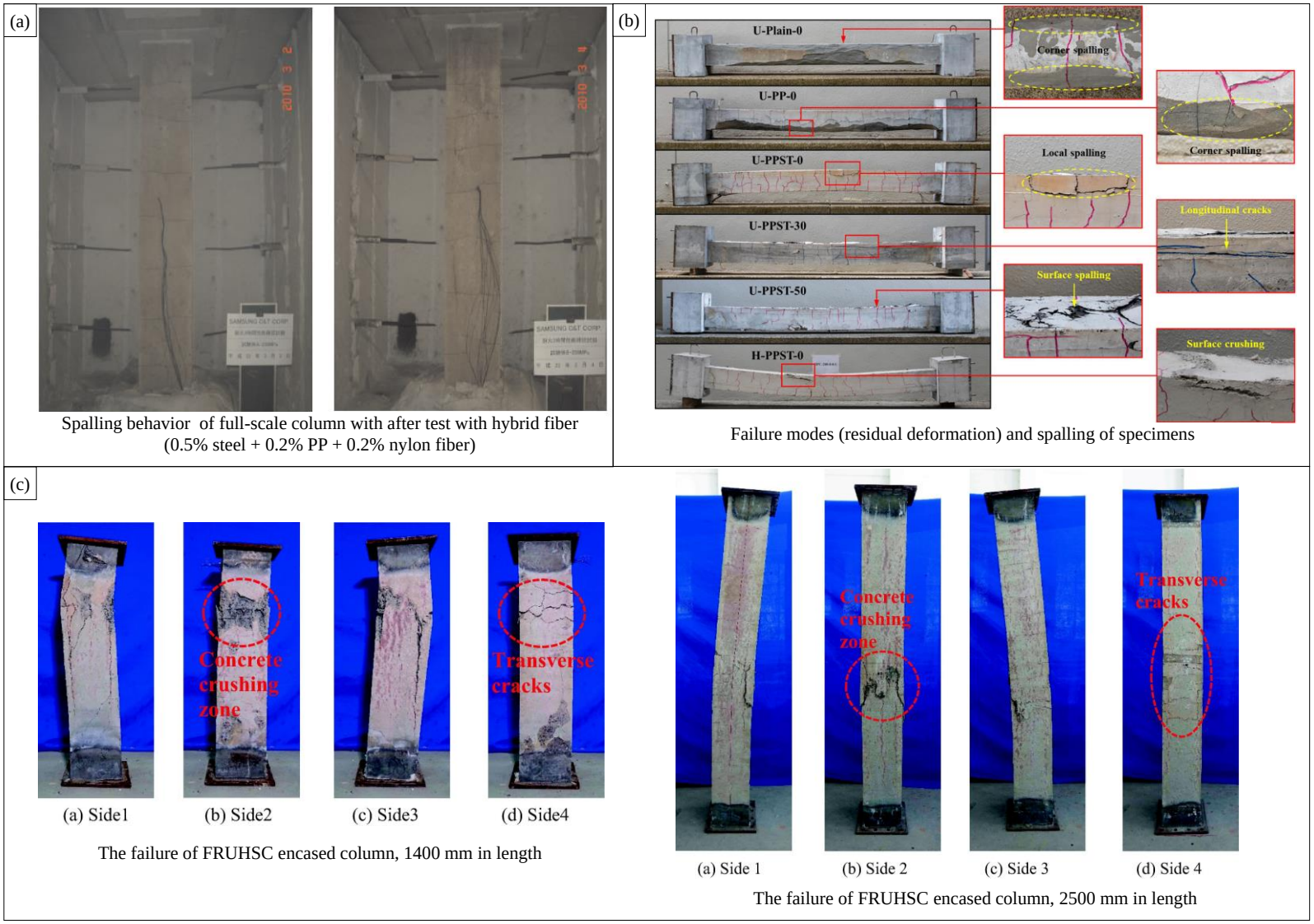

Fig. 33 – Spalling behavior of UHPC columns at elevated temperature: (a) Lee, et al. [22]; (b) Li, et al. [61]; and (c) Du, et al. [31]

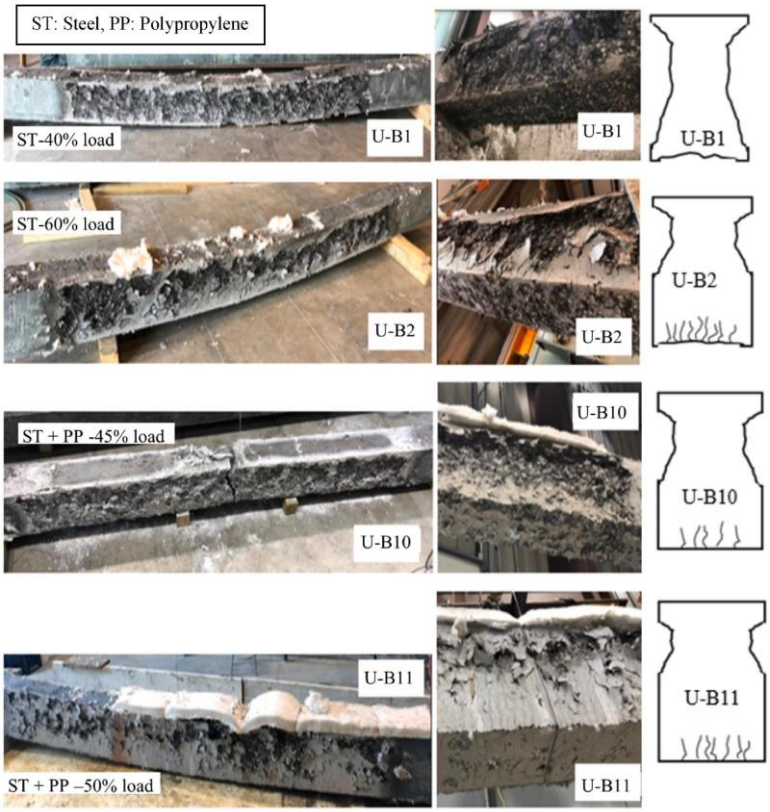

Fig. 34 – Fire test results [63];: (a) fiber-reinforced UHPC beams after exposure to fire, (b) bottom surface of beams, (c) schematic representation of cracking pattern and spalling of beams

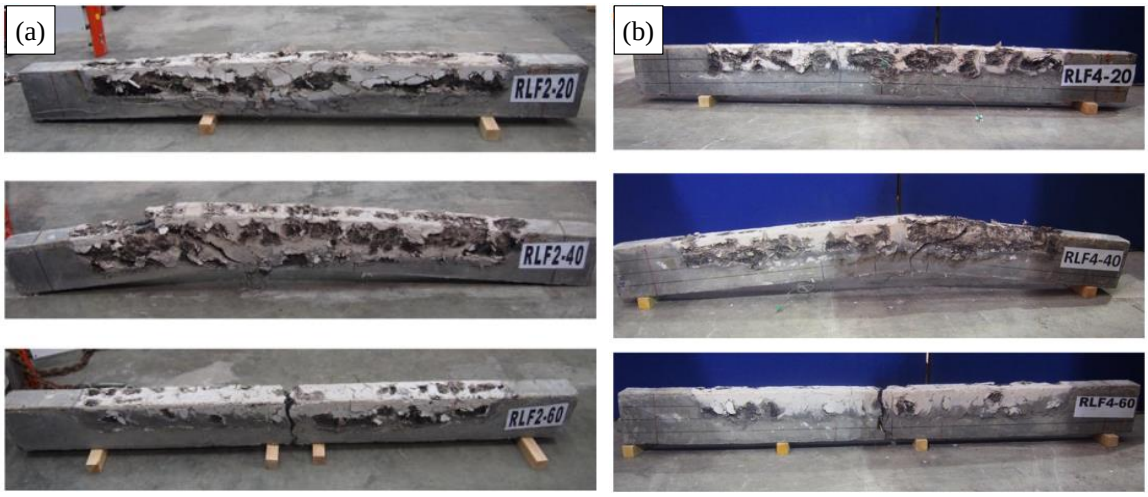

Beams with 2% steel fiber content

Beams with 4% steel fiber content

Hybrid fibers beam containing 2% steel and 0.4% polypropylene fibers after fire test

Fig. 35 – Spalling behavior of beams [64]

- A higher content of single-length steel fiber (2%-4%) reduces spalling intensity and improves spalling in full-scale UHPC columns. Single-length PP fibers, even at higher than Eurocode 2 dosage, do not prevent spalling. However, the use of hybrid steel and PP fiber in large-scale columns prevents spalling even with less PP fiber dosage than recommended in Eurocode 2. Hybrid fibers also reduce spalling in UHPC beams, improving their structural performance under elevated temperatures.

6.2 Research prospective

To fully understand the role of fiber-reinforced UHPC under fire, further investigations are required. Currently, there is a lack of consensus on the material and structural behavior of fiber-reinforced UHPC at high temperatures. Future research should focus on the following areas:

- The effect of hybrid fibers on the spalling performance of UHPC varies depending on the type and quantity of fibers used. It is essential to establish clear guidelines for the minimum and maximum content of various fibers to achieve improved spalling performance at elevated temperatures without compromising mechanical strength and durability.
- Existing research on the spalling performance of UHPC under high temperatures mainly focuses on the volume of natural fibers used. However, the mechanical properties of fibers, such as aspect ratio, volume, and coefficient of thermal expansion, also play a crucial role. Therefore, further studies are required to standardize the appropriate natural fiber type, volume, fiber length, aspect ratio, and coefficient of thermal expansion in UHPC, particularly for hybrid fibers.
- The current regulations in Eurocode 2 may not be adequate for UHPC, and additional precise instructions are necessary, including the appropriate dosage of various types of fibers for specific aspect ratios and matrix compositions. Although Eurocode 2 specifies a minimum volume of propylene fibers to minimize the risk of spalling in high-strength concrete, it is essential to note that spalling resistance depends on the aspect ratio and volume of fibers and the cementitious matrix constituents, particularly in the case of UHPC.
- Further studies are required to determine the influence of specimen size, heating rate, drying method, and cooling method on UHPC's behavior under fire. The available information on these factors is inconsistent, and developing a standardized testing procedure is necessary to minimize their impact on the outcome of UHPC under elevated temperatures.
- The research available on UHPC reinforced with PVA or PE fibers is insufficient to draw conclusive statements on their strain hardening behavior at elevated temperatures. Achieving strain-hardening behavior under fire for these fibers remains a challenging task, necessitating further investigation.
- To fully understand the synergetic effect of hybrid fibers, quantitative analysis/characterization of percolation is necessary. X-ray Computed Tomography is a promising tool for achieving this goal in the future.
- An in-depth study is required to improve the spalling behavior of UHPC with hybrid steel and natural fibers, promoting its use as a sustainable material for elevated temperatures. Future studies should focus on the MIP analysis of natural fibers in UHPC to understand their swelling/shrink effect, which can influence pore size/diameter at high temperatures.
- Large-scale testing of UHPC structures is necessary to identify experimental phenomena before practical implementation, particularly with the use of hybrid fibers. However, there is a lack of codes/standards for testing and heating full-scale members under high temperatures. To strengthen existing RC structures with UHPC, new design provisions must be established.
- Fiber-reinforced UHPC's is made up of many constituents that require the development of new ideas and theories to understand the spalling phenomenon and its characteristics under elevated

temperatures. Analytical models and equations with reasonable assumptions can also aid in understanding the high-temperature behavior of fiber-reinforced UHPC. Future research should include numerical modeling of the structural behavior of fiber-reinforced UHPC at high temperatures.

- Further investigation is required to understand the spalling of full-scale fiber-reinforced UHPC beams/slabs in fire-resistant construction, considering various aspects such as the addition of fiber reinforcement and their mechanism. The repair/strengthening of a damaged structural member after exposure to fire with a new type of fire-resistant fiber-reinforced UHPC material is a new consideration.

CRediT authorship contribution statement

Mehran Khan: Conceptualization, Methodology, Investigation, Formal analysis, Writing–original draft, Writing–review & editing. **Mingfeng Kai:** Visualization, Methodology, Writing–review & editing. **Muhammad Riaz Ahmad:** Visualization, Methodology, Writing–review & editing. **Jiancong Lao:** Data Curation, Resources, Validation. **Jian-Guo Dai:** Conceptualization, Funding acquisition, Project administration, Writing–review & editing, Supervision.

Declaration of Competing Interest

The authors declare that they have no known competing financial interests or personal relationships that could have appeared to influence the work reported in this paper.

Acknowledgment

The financial support for the first authors from the Postdoc Matching Fund Scheme (Project codes: P0014094 and P0005306) at The Hong Kong Polytechnic University is gratefully acknowledged.

References

[1] Huang, B.-T.; Wu, J.-Q.; Yu, J.; Dai, J.-G.; Leung, C.K.; and Li, V.C. (2021) "Seawater sea-sand engineered/strain-hardening cementitious composites (ECC/SHCC): Assessment and modeling of crack characteristics," Cement and Concrete Research, 140, pp. 106292.

[2] De la Varga, I.; and Graybeal, B.A. (2015) "Dimensional stability of grout-type materials used as connections between prefabricated concrete elements," Journal of Materials in Civil Engineering, 27(9), pp. 04014246.

[3] Meng, Q.; Wu, C.; Li, J.; Liu, Z.; Wu, P.; Yang, Y.; and Wang, Z. (2020) "Steel/basalt rebar reinforced Ultra-High Performance Concrete components against methane-air explosion loads," Composites Part B: Engineering, 198, pp. 108215.

[4] Li, P.; Sluijsmans, M.J.; Brouwers, H.; and Yu, Q. (2020) "Functionally graded ultra-high performance cementitious composite with enhanced impact properties," Composites Part B: Engineering, 183, pp. 107680.

[5] Lao, J.-C.; Huang, B.-T.; Xu, L.-Y.; Khan, M.; Fang, Y.; and Dai, J.-G. (2023) "Seawater sea-sand Engineered Geopolymer Composites (EGC) with high strength and high ductility," Cement and Concrete Composites, 138, pp. 104998.

[6] Lao, J.-C.; Xu, L.-Y.; Huang, B.-T.; Zhu, J.-X.; Khan, M.; and Dai, J.-G. (2023) "Utilization of sodium carbonate activator in strain-hardening ultra-high-performance geopolymer concrete (SH-UHPGC)," Frontiers in Materials, 10, pp. 1-12.

[7] Lao, J.-C.; Huang, B.-T.; Fang, Y.; Xu, L.-Y.; Dai, J.-G.; and Shah, S.P. (2023) "Strain-hardening alkali-activated fly ash/slag composites with ultra-high compressive strength and ultra-high tensile ductility," Cement and Concrete Research, 165, pp. 107075.

[8] Khan, M.; Lao, J.; and Dai, J.-G. (2022) "Comparative study of advanced computational techniques for estimating the compressive strength of UHPC," J. Asian Concr. Fed, 8, pp. 51-68.

[9] Khan, M.; Lao, J.; Ahmad, M.R.; Kai, M.-F.; and Dai, J.-G. (2023) "The role of calcium aluminate cement in developing an efficient ultra-high performance concrete resistant to explosive spalling under high temperatures," Construction and Building Materials, 384, pp. 131469.

[10] Ahmad, S.; Rasul, M.; Adekunle, S.K.; Al-Dulaijan, S.U.; Maslehuddin, M.; and Ali, S.I. (2019) "Mechanical properties of steel

fiber-reinforced UHPC mixtures exposed to elevated temperature: Effects of exposure duration and fiber content," Composites Part B: Engineering, 168, pp. 291-301.
[11] Perry, V., What really is ultra-high performance concrete?–Towards a global definition, The 2nd International Conference on Ultra-High Performance Concrete Material & Structures, 2018, pp. 7-10.
[12] ACI, A. (2018) "239R-18: Ultra-High Performance Concrete: An Emerging Technology Report (2018)," American Concrete Institute: Farmington Hills, MI, USA, pp.
[13] Russell, H.G.; Graybeal, B.A.; and Russell, H.G., Ultra-high performance concrete: A state-of-the-art report for the bridge community, United States. Federal Highway Administration. Office of Infrastructure …, 2013.
[14] Qian, Y.; Yang, D.; Xia, Y.; Gao, H.; and Ma, Z. (2021) "Transport Properties and Resistance Improvement of Ultra-High Performance Concrete (UHPC) after Exposure to Elevated Temperatures," Buildings, 11(9), pp. 416.
[15] Pokorný, P.; Kolísko, J.; Čítek, D.; and Kostelecká, M. (2020) "Effect of elevated temperature on the bond strength of prestressing reinforcement in UHPC," Materials, 13(21), pp. 4990.
[16] Missemer, L.; Ouedraogo, E.; Malecot, Y.; Clergue, C.; and Rogat, D. (2019) "Fire spalling of ultra-high performance concrete: From a global analysis to microstructure investigations," Cement and Concrete Research, 115, pp. 207-219.
[17] Li, Y. (2021) "Effect of post-fire curing and silica fume on permeability of ultra-high performance concrete," Construction and Building Materials, 290, pp. 123175.
[18] Kodur, V.; Banerji, S.; and Solhmirzaei, R. (2020) "Effect of temperature on thermal properties of ultrahigh-performance concrete," Journal of Materials in Civil Engineering, 32(8), pp. 04020210.
[19] Liu, J.-C.; Tan, K.H.; and Yao, Y. (2018) "A new perspective on nature of fire-induced spalling in concrete," Construction and Building Materials, 184, pp. 581-590.
[20] Zhang, D.; Liu, Y.; and Tan, K.H. (2021) "Spalling resistance and mechanical properties of strain-hardening ultra-high performance concrete at elevated temperature," Construction and Building Materials, 266, pp. 120961.
[21] Choe, G.; Kim, G.; Gucunski, N.; and Lee, S. (2015) "Evaluation of the mechanical properties of 200 MPa ultra-high-strength concrete at elevated temperatures and residual strength of column," Construction and Building Materials, 86, pp. 159-168.
[22] Lee, J.-H.; Sohn, Y.-S.; and Lee, S.-H. (2012) "Fire resistance of hybrid fibre-reinforced, ultra-high-strength concrete columns with compressive strength from 120 to 200 MPa," Magazine of Concrete Research, 64(6), pp. 539-550.
[23] Li, Y.; Pimienta, P.; Pinoteau, N.; and Tan, K.H. (2019) "Effect of aggregate size and inclusion of polypropylene and steel fibers on explosive spalling and pore pressure in ultra-high-performance concrete (UHPC) at elevated temperature," Cement and Concrete Composites, 99, pp. 62-71.
[24] Bangi, M.R.; and Horiguchi, T. (2011) "Pore pressure development in hybrid fibre-reinforced high strength concrete at elevated temperatures," Cement and Concrete Research, 41(11), pp. 1150-1156.
[25] Kodur, V.; Cheng, F.-P.; Wang, T.-C.; and Sultan, M. (2003) "Effect of strength and fiber reinforcement on fire resistance of high-strength concrete columns," Journal of Structural Engineering, 129(2), pp. 253-259.
[26] Park, J.-J.; Yoo, D.-Y.; Kim, S.; and Kim, S.-W. (2019) "Benefits of synthetic fibers on the residual mechanical performance of UHPFRC after exposure to ISO standard fire," Cement and Concrete Composites, 104, pp. 103401.
[27] Zhang, D.; Tan, K.H.; Dasari, A.; and Weng, Y. (2020) "Effect of natural fibers on thermal spalling resistance of ultra-high performance concrete," Cement and Concrete Composites, 109, pp. 103512.
[28] Ozawa, M.; Bo, Z.; Kawaguchi, J.; and Uchida, Y., Preventive effect on spalling of UFC using jute fiber at high temperature, MATEC web of conferences, EDP Sciences, 2013, p. 02006.
[29] Ozawa, M.; Parajuli, S.S.; Uchida, Y.; and Zhou, B. (2019) "Preventive effects of polypropylene and jute fibers on spalling of UHPC at high temperatures in combination with waste porous ceramic fine aggregate as an internal curing material," Construction and Building Materials, 206, pp. 219-225.

[30] Ren, G.; Gao, X.; and Zhang, H. (2022) "Utilization of hybrid sisal and steel fibers to improve elevated temperature resistance of ultra-high performance concrete," Cement and Concrete Composites, 130, pp. 104555.
[31] Du, Y.; Qi, H.-H.; Huang, S.-S.; and Liew, J.R. (2020) "Experimental study on the spalling behaviour of ultra-high strength concrete in fire," Construction and Building Materials, 258, pp. 120334.
[32] Zhang, D.; Tan, G.Y.; and Tan, K.H. (2021) "Combined effect of flax fibers and steel fibers on spalling resistance of ultra-high performance concrete at high temperature," Cement and Concrete Composites, 121, pp. 104067.
[33] Liang, X.; Wu, C.; Su, Y.; Chen, Z.; and Li, Z. (2018) "Development of ultra-high performance concrete with high fire resistance," Construction and Building Materials, 179, pp. 400-412.
[34] Zhang, D.; and Tan, K.H. (2020) "Effect of various polymer fibers on spalling mitigation of ultra-high performance concrete at high temperature," Cement and Concrete Composites, 114, pp. 103815.
[35] Zhang, D.; Zhang, Y.; Dasari, A.; Tan, K.H.; and Weng, Y. (2021) "Effect of spatial distribution of polymer fibers on preventing spalling of UHPC at high temperatures," Cement and Concrete Research, 140, pp. 106281.
[36] Cai, R.; Liu, J.-C.; and Ye, H. (2021) "Spalling Prevention of Ultrahigh-Performance Concrete: Comparative Effectiveness of Polyethylene Terephthalate and Polypropylene Fibers," Journal of Materials in Civil Engineering, 33(12), pp. 04021344.
[37] Li, Y.; Tan, K.H.; and Yang, E.-H. (2019) "Synergistic effects of hybrid polypropylene and steel fibers on explosive spalling prevention of ultra-high performance concrete at elevated temperature," Cement and Concrete Composites, 96, pp. 174-181.
[38] Khoury, G.; and Willoughby, B. (2008) "Polypropylene fibres in heated concrete. Part 1: Molecular structure and materials behaviour," Magazine of concrete research, 60(2), pp. 125-136.
[39] Li, Y.; Tan, K.H.; and Yang, E.-H. (2018) "Influence of aggregate size and inclusion of polypropylene and steel fibers on the hot permeability of ultra-high performance concrete (UHPC) at elevated temperature," Construction and Building Materials, 169, pp. 629-637.
[40] Li, Y.; Yang, E.-H.; Zhou, A.; and Liu, T. (2021) "Pore pressure build-up and explosive spalling in concrete at elevated temperature: A review," Construction and Building Materials, 284, pp. 122818.
[41] Zhu, Y.; Hussein, H.; Kumar, A.; and Chen, G. (2021) "A review: Material and structural properties of UHPC at elevated temperatures or fire conditions," Cement and Concrete Composites, 123, pp. 104212.
[42] Ozawa, M.; and Morimoto, H. (2014) "Effects of various fibres on high-temperature spalling in high-performance concrete," Construction and Building Materials, 71, pp. 83-92.
[43] Bian, H.; Hannawi, K.; Takarli, M.; Molez, L.; and Prince, W. (2016) "Effects of thermal damage on physical properties and cracking behavior of ultrahigh-performance fiber-reinforced concrete," Journal of Materials Science, 51(22), pp. 10066-10076.
[44] Zhang, D.; Dasari, A.; and Tan, K.H. (2018) "On the mechanism of prevention of explosive spalling in ultra-high performance concrete with polymer fibers," Cement and Concrete Research, 113, pp. 169-177.
[45] Abyaneh, S.D.; Wong, H.; and Buenfeld, N. (2016) "Simulating the effect of microcracks on the diffusivity and permeability of concrete using a three-dimensional model," Computational Materials Science, 119, pp. 130-143.
[46] Liang, X.; Wu, C.; Yang, Y.; and Li, Z. (2019) "Experimental study on ultra-high performance concrete with high fire resistance under simultaneous effect of elevated temperature and impact loading," Cement and Concrete Composites, 98, pp. 29-38.
[47] Xiong, M.-X.; and Liew, J.R. (2015) "Spalling behavior and residual resistance of fibre reinforced Ultra-High performance concrete after exposure to high temperatures," Materiales de Construcción, 65(320), pp. e071-e071.
[48] Yang, J.; Peng, G.-F.; Zhao, J.; and Shui, G.-S. (2019) "On the explosive spalling behavior of ultra-high performance concrete with and without coarse aggregate exposed to high temperature," Construction and Building Materials, 226, pp. 932-944.

[49] Wu, Z.; Shi, C.; He, W.; and Wu, L. (2016) "Effects of steel fiber content and shape on mechanical properties of ultra high performance concrete," Construction and building materials, 103, pp. 8-14.
[50] Abdallah, S.; Fan, M.; and Cashell, K. (2017) "Bond-slip behaviour of steel fibres in concrete after exposure to elevated temperatures," Construction and Building Materials, 140, pp. 542-551.
[51] Li, Y.; Yang, E.-H.; and Tan, K.H. (2020) "Flexural behavior of ultra-high performance hybrid fiber reinforced concrete at the ambient and elevated temperature," Construction and Building Materials, 250, pp. 118487.
[52] Deshpande, A.A.; Kumar, D.; and Ranade, R. (2019) "Influence of high temperatures on the residual mechanical properties of a hybrid fiber-reinforced strain-hardening cementitious composite," Construction and Building Materials, 208, pp. 283-295.
[53] Luo, J.; Cai, Z.; Yu, K.; Zhu, W.; and Lu, Z. (2019) "Temperature impact on the micro-structures and mechanical properties of high-strength engineered cementitious composites," Construction and Building Materials, 226, pp. 686-698.
[54] Habel, K.; Viviani, M.; Denarié, E.; and Brühwiler, E. (2006) "Development of the mechanical properties of an ultra-high performance fiber reinforced concrete (UHPFRC)," Cement and Concrete Research, 36(7), pp. 1362-1370.
[55] Wang, X.H.; Jacobsen, S.; He, J.Y.; Zhang, Z.L.; Lee, S.F.; and Lein, H.L. (2009) "Application of nanoindentation testing to study of the interfacial transition zone in steel fiber reinforced mortar," Cement and Concrete Research, 39(8), pp. 701-715.
[56] Wu, Z.; Shi, C.; and Khayat, K. (2016) "Influence of silica fume content on microstructure development and bond to steel fiber in ultra-high strength cement-based materials (UHSC)," Cement and Concrete Composites, 71, pp. 97-109.
[57] Noumowe, A. (2005) "Mechanical properties and microstructure of high strength concrete containing polypropylene fibres exposed to temperatures up to 200 C," Cement and concrete research, 35(11), pp. 2192-2198.
[58] Kahanji, C.; Ali, F.; Nadjai, A.; and Alam, N. (2018) "Effect of curing temperature on the behaviour of UHPFRC at elevated temperatures," Construction and Building Materials, 182, pp. 670-681.
[59] Suescum-Morales, D.; Ríos, J.D.; Martínez-De La Concha, A.; Cifuentes, H.; Jiménez, J.R.; and Fernández, J.M. (2021) "Effect of moderate temperatures on compressive strength of ultra-high-performance concrete: A microstructural analysis," Cement and Concrete Research, 140, pp. 106303.
[60] Zhu, Y.; Zhang, Y.; Hussein, H.H.; and Chen, G. (2020) "Flexural strengthening of reinforced concrete beams or slabs using ultra-high performance concrete (UHPC): A state of the art review," Engineering Structures, 205, pp. 110035.
[61] Li, Y.; Du, P.; and Tan, K.H. (2021) "Fire resistance of ultra-high performance concrete columns subjected to axial and eccentric loading," Engineering Structures, 248, pp. 113158.
[62] Eurocode 2, C. (2004) "2: Design of Concrete Structures—Part 1–2: General Rules—Structural Fire Design," European Standard: London, UK, pp.
[63] Banerji, S.; Kodur, V.; and Solhmirzaei, R. (2020) "Experimental behavior of ultra high performance fiber reinforced concrete beams under fire conditions," Engineering Structures, 208, pp. 110316.
[64] Kahanji, C.; Ali, F.; and Nadjai, A. (2016) "Explosive spalling of ultra-high performance fibre reinforced concrete beams under fire," Journal of Structural Fire Engineering, 7(4), pp.
[65] Qin, H.; Yang, J.; Yan, K.; Doh, J.-H.; Wang, K.; and Zhang, X. (2021) "Experimental research on the spalling behaviour of ultra-high performance concrete under fire conditions," Construction and Building Materials, 303, pp. 124464.